

Probing Jet Suppression with Pairs of Jets in ATLAS

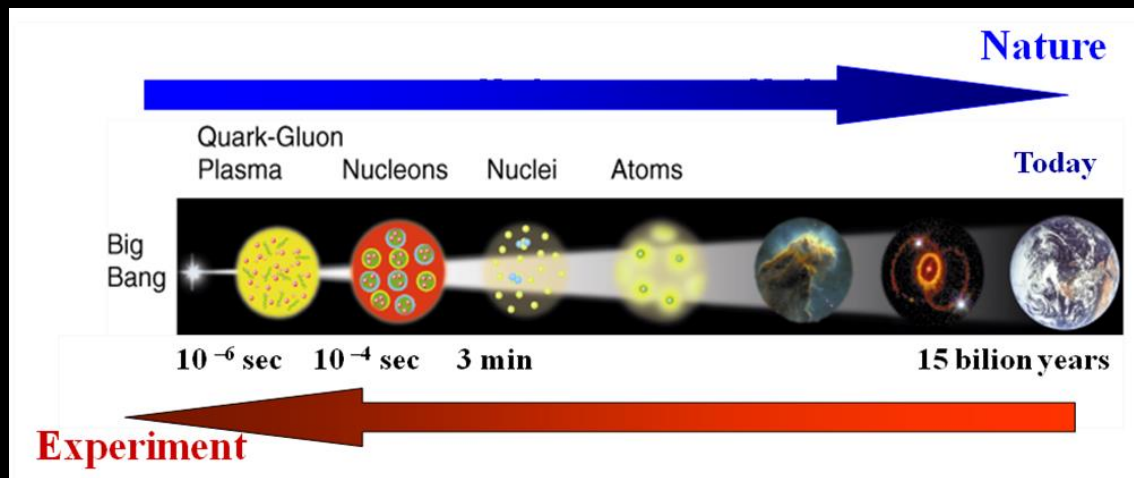
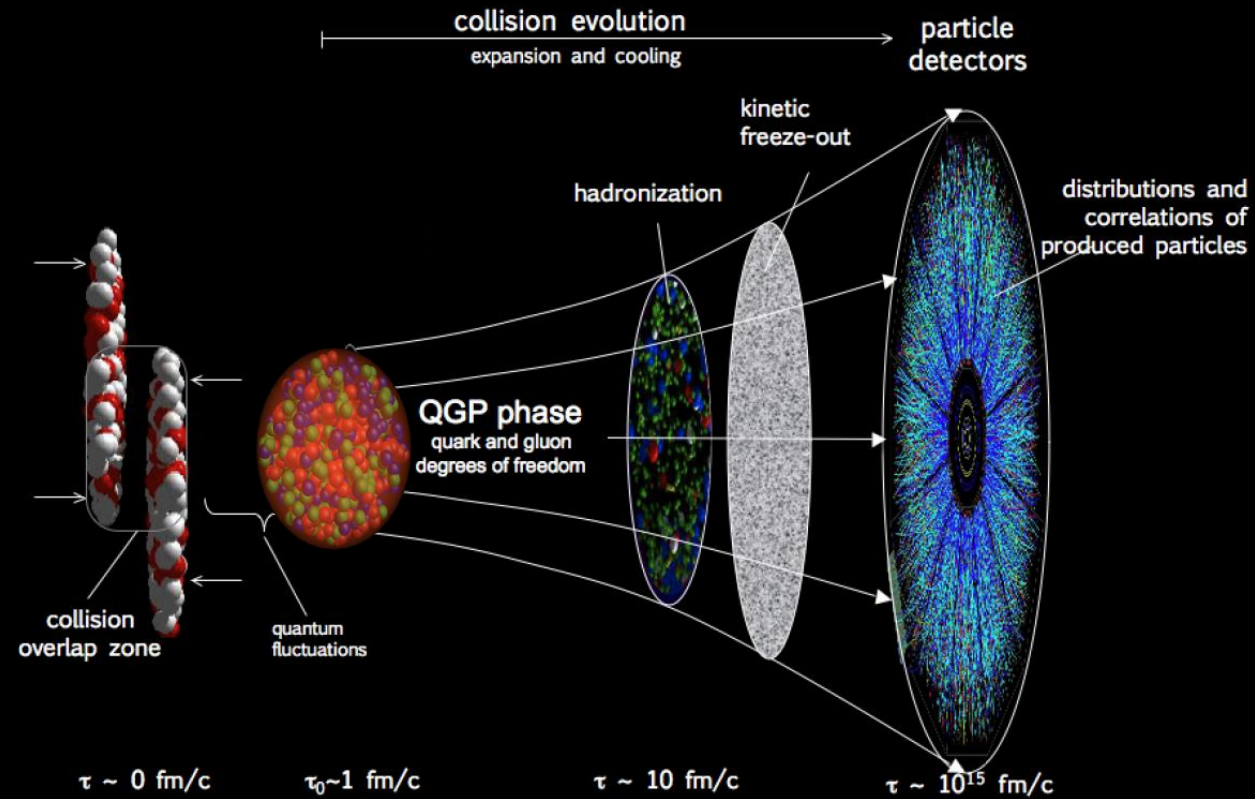
Timothy Rinn

Discussing new ATLAS results documented at: <https://atlas.web.cern.ch/Atlas/GROUPS/PHYSICS/PAPERS/HION-2019-02/>

QGP in Heavy Ion Collisions

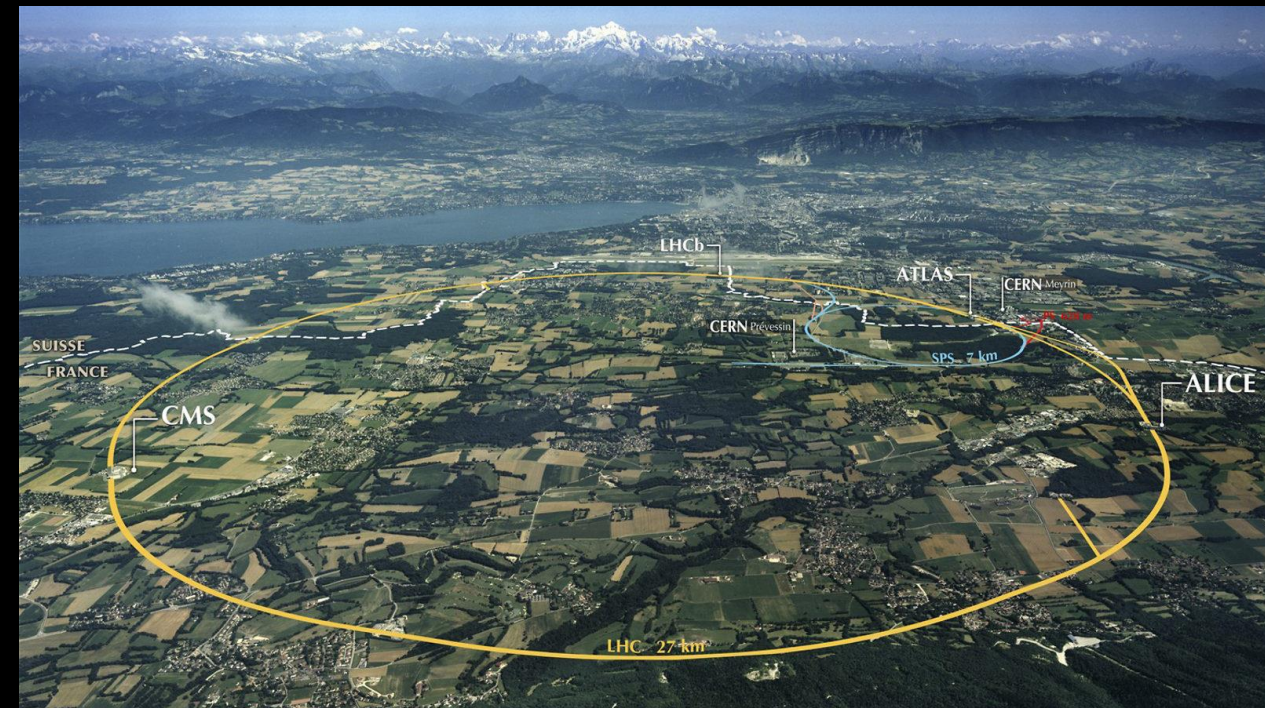
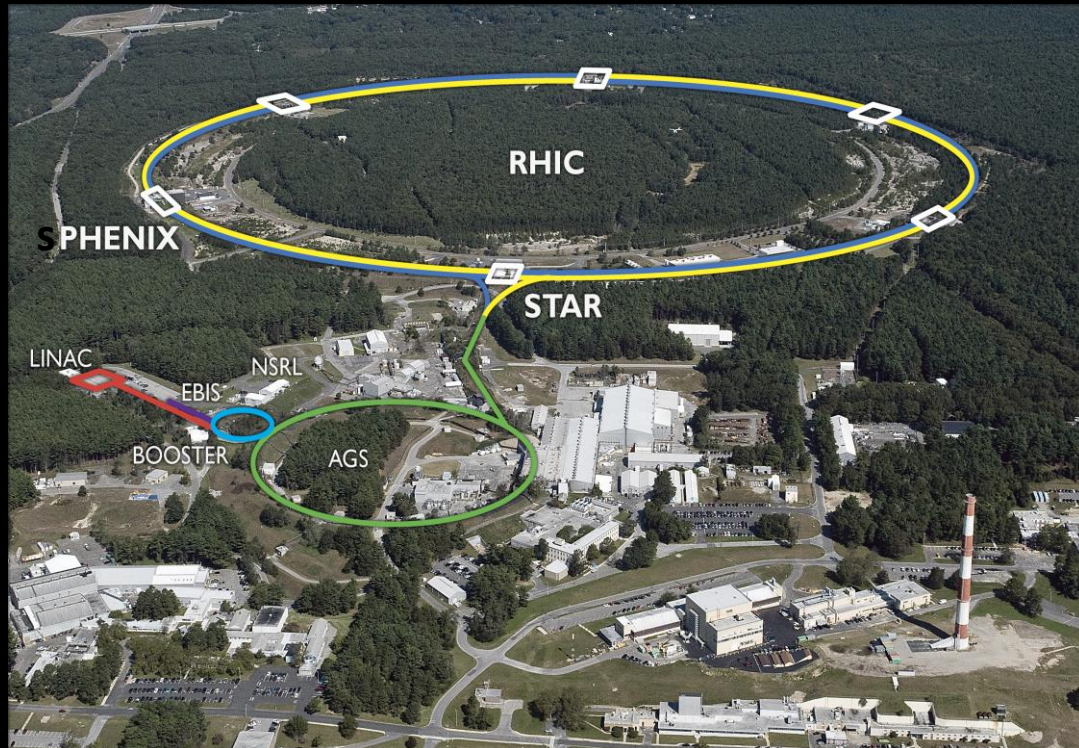
Heavy ion collisions enable the creation of a high density and temperature medium to study strong force interactions in conditions similar to those of the early universe

Nuclear collisions and the QGP expansion



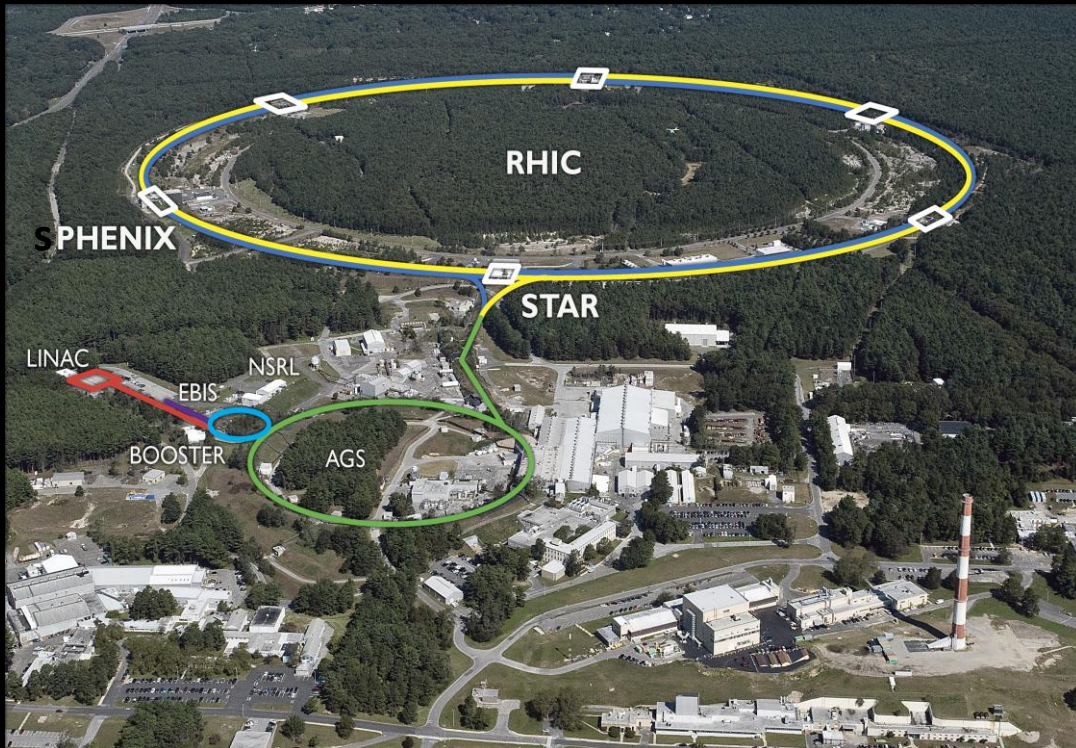
Producing the QGP in laboratories:

- Two collider facilities
 - Relativistic Heavy Ion Collider on Long Island New York
 - The Large Hadron Collider at CERN in Switzerland/France



Producing the QGP in laboratories:

- Two collider facilities
 - Relativistic Heavy Ion Collider on Long Island New York
 - The Large Hadron Collider at CERN in Switzerland/France

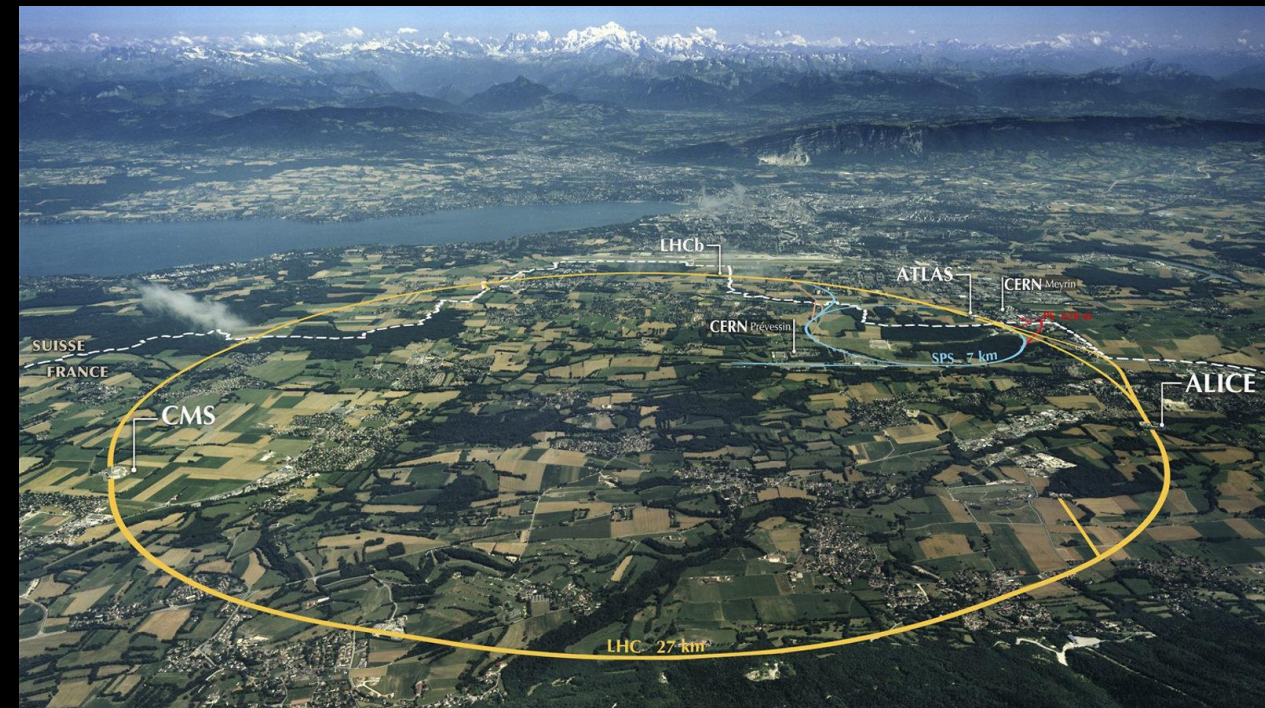


- Specifically designed for the study of heavy ion collisions
- Versatile Colliding facility!
 - Collides a vast range of nuclei:
 - Au+Au, Cu+Cu, d+Au, U+U, p+Au, He³+Au
 - Capable of producing transversely polarized proton beams
- Tunable “low” collision energy of ≤ 200 GeV
- Produces a Quark Gluon Plasma with $T \sim 220$ MeV

Producing the QGP in laboratories:

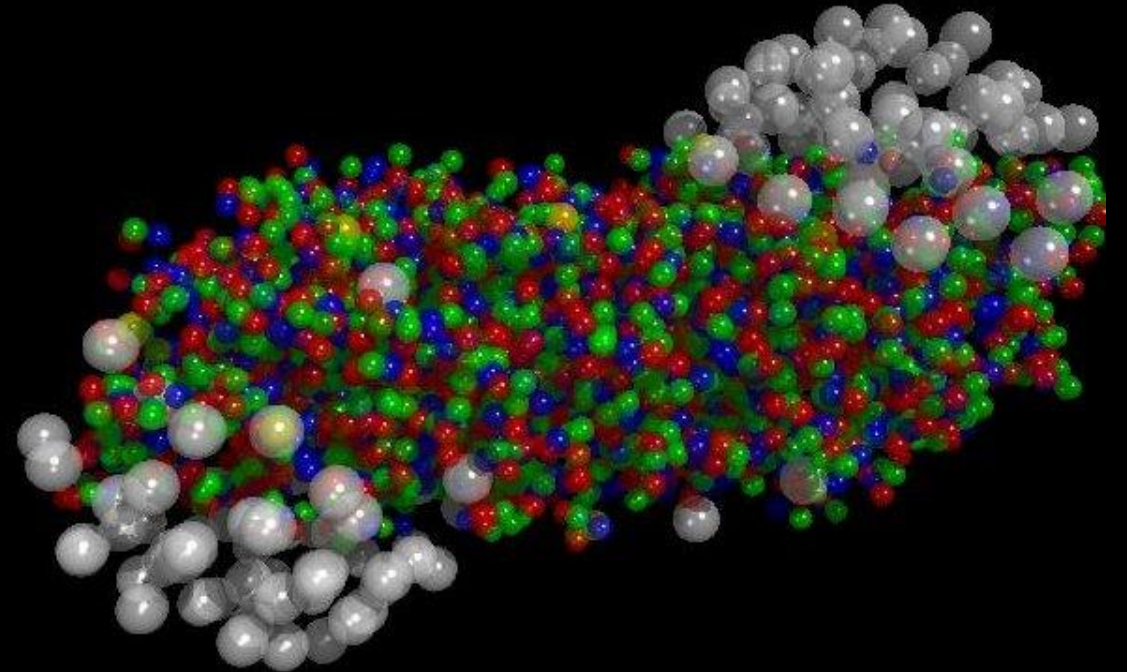
- Two collider facilities
 - Relativistic heavy Ion Collider on Long Island New York
 - The Large Hadron Collider at CERN in Switzerland/France

- Joint facility for high energy particle and heavy ion physics
 - Share running time between Particle and Nuclear physics efforts
- High luminosity collider facility
 - ~ 30 kHz event rate in Pb+Pb
 - Run3 will enable 50 kHz running
- High collision energy of 5.02 TeV
 - Produces a QGP with $T \sim 300$ MeV



Probing the properties of the QGP

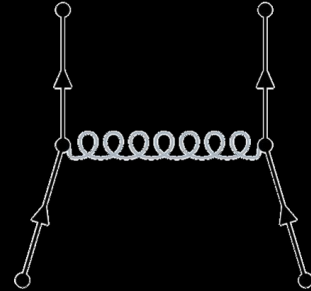
- In order to understand the properties of interactions within the QGP we utilize a variety of probes:
 - High p_T probes, such as jets of high p_T particles
 - Probes with a variety of masses:
 - heavy flavor quarks
 - Correlations of particles



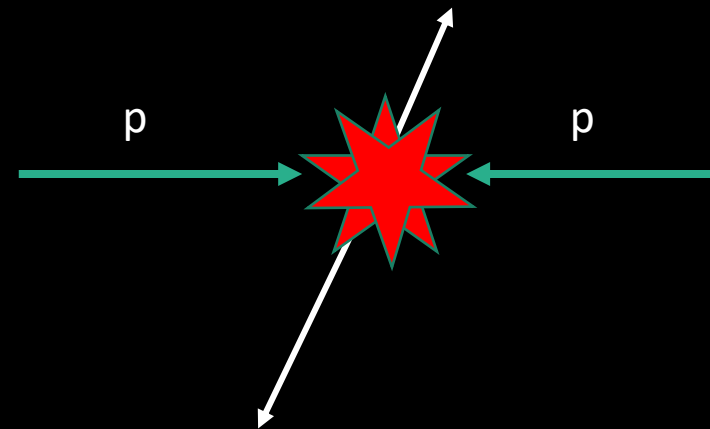
QCD jets

Produced in large momentum transfer QCD interactions:

- Such as:
 $q + q \rightarrow q + q$



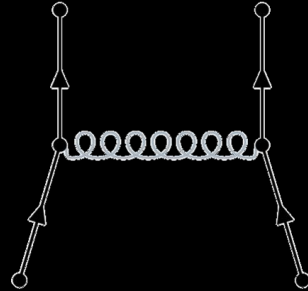
- Calculable using perturbative techniques



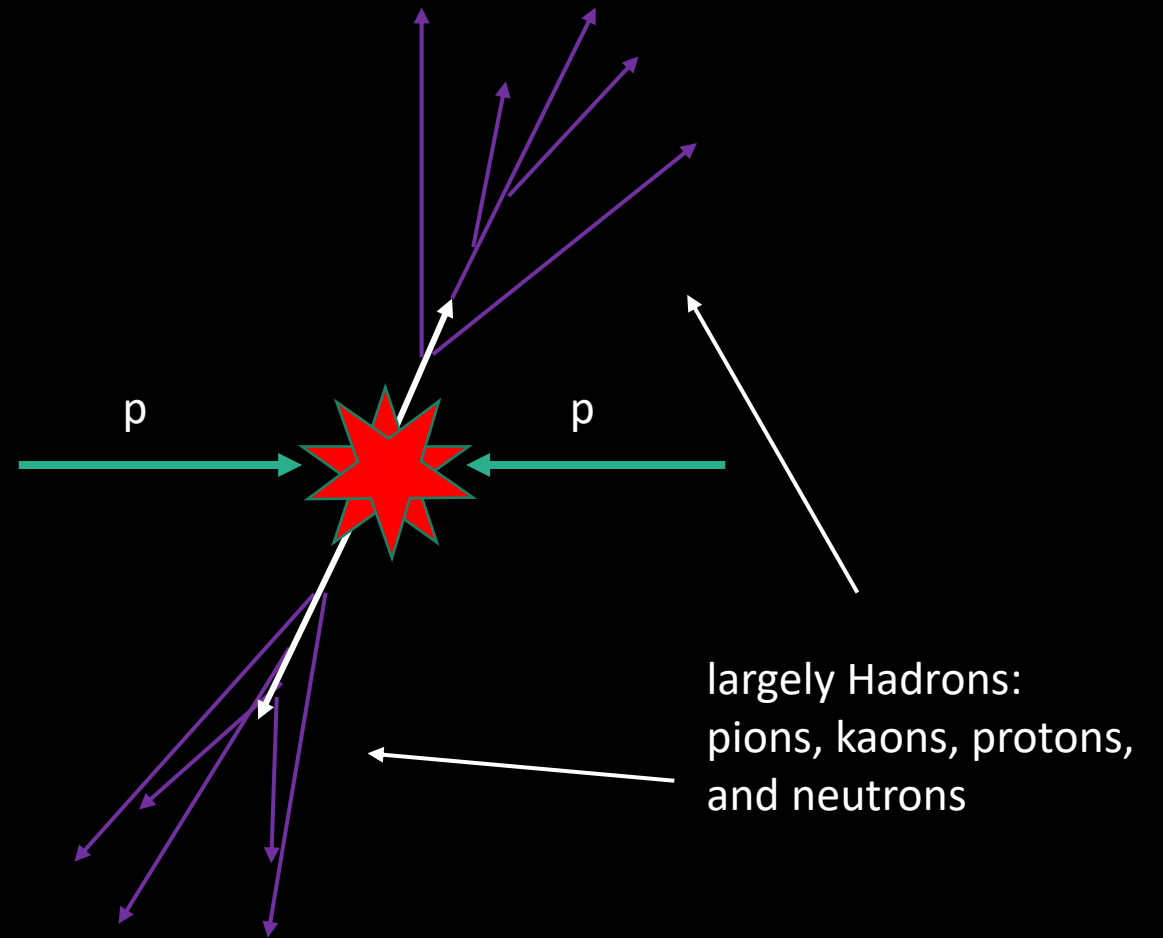
QCD jets

Produced in large momentum transfer QCD interactions:

- Such as:
 $q + q \rightarrow q + q$



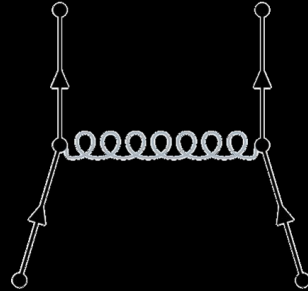
- Calculable using perturbative techniques
- Initial produced quarks/gluons evolve into a particle shower through fragmentation and hadronization



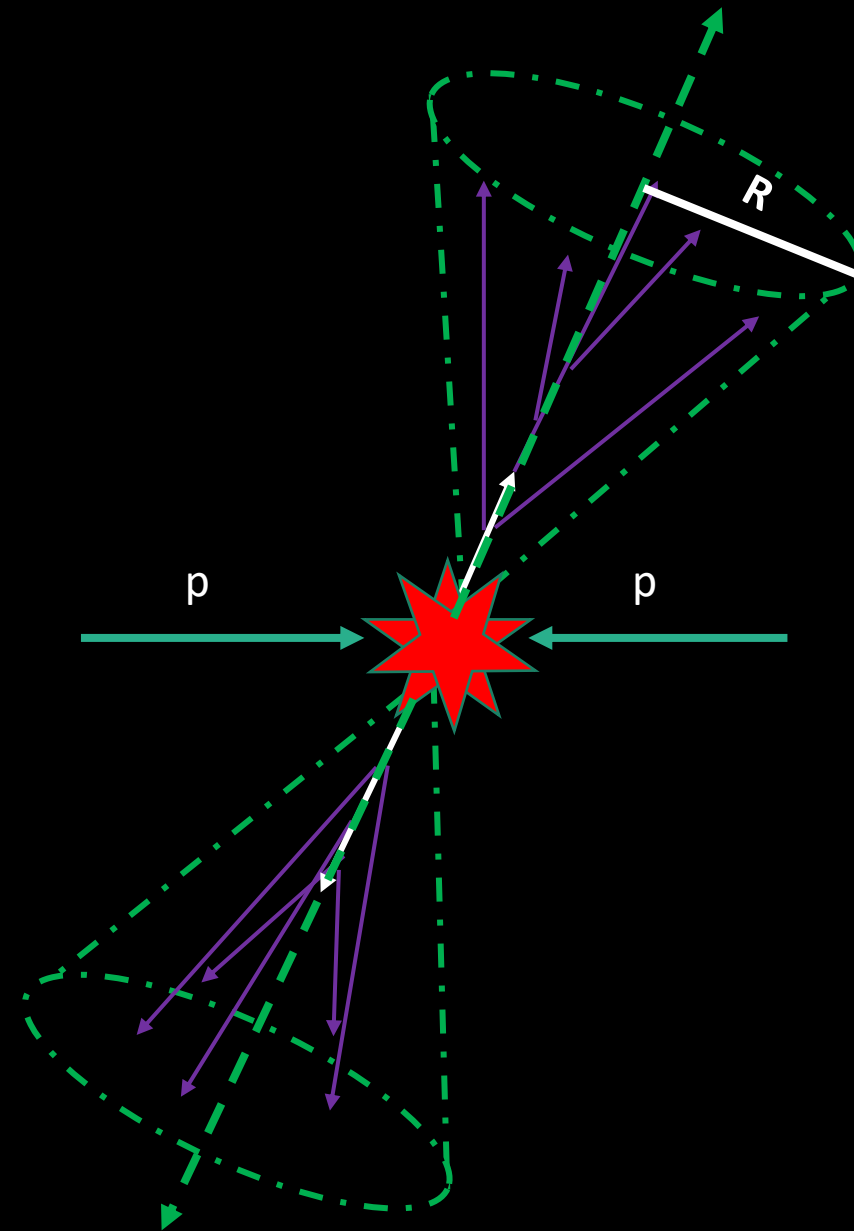
QCD jets

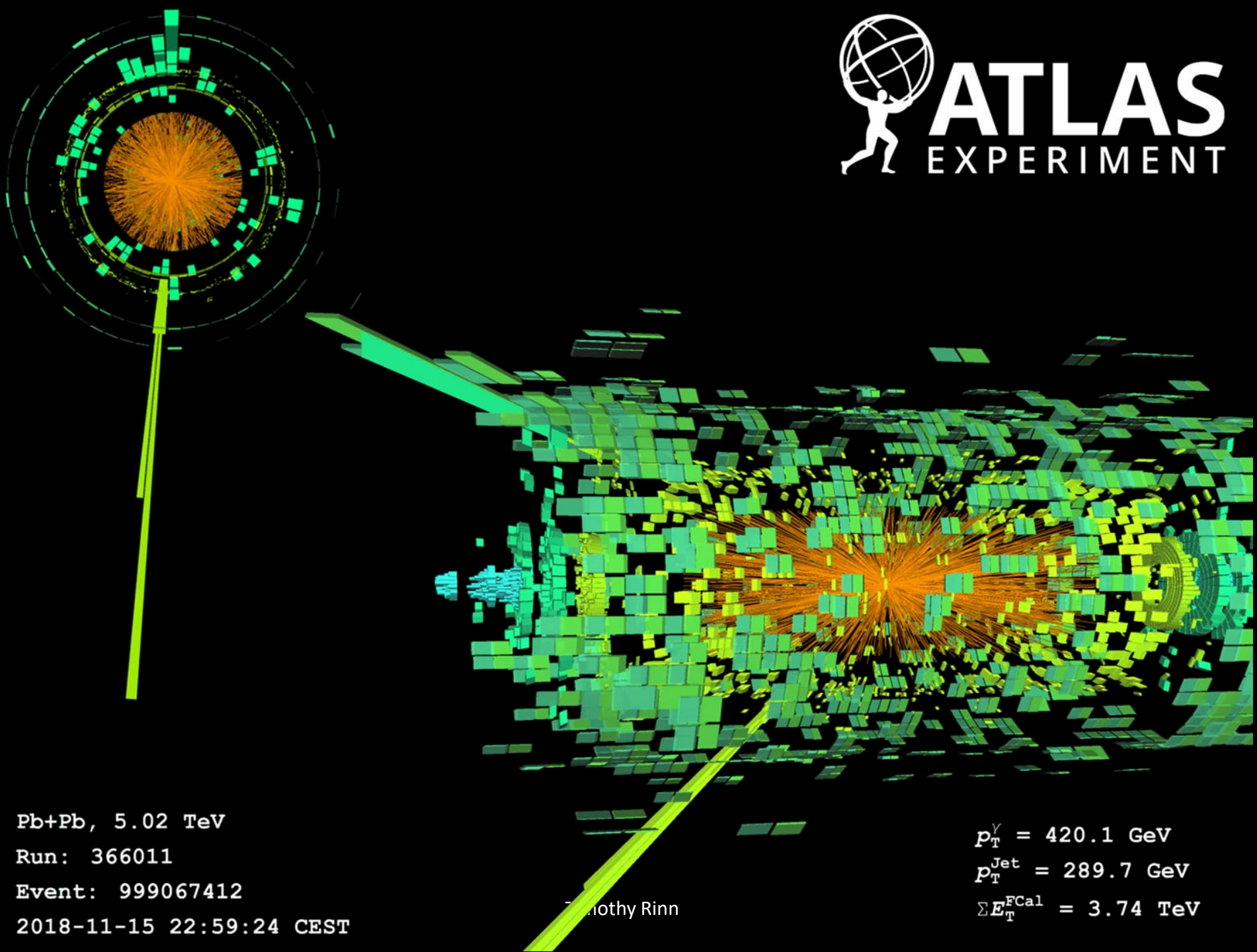
Produced in large momentum transfer QCD interactions:

- Such as:
 $q + q \rightarrow q + q$



- Calculable using perturbative techniques
- Initial produced quarks/gluons evolve into a particle shower through fragmentation and hadronization
- Final state particles grouped into jets using “jet finding algorithms”





Pb+Pb, 5.02 TeV

Run: 366011

Event: 999067412

2018-11-15 22:59:24 CEST

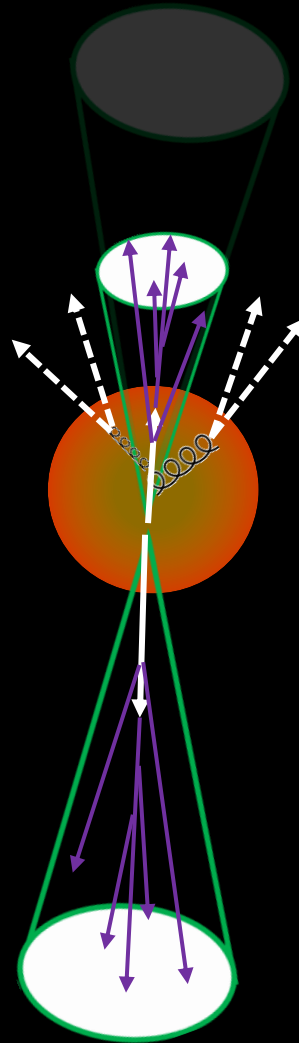
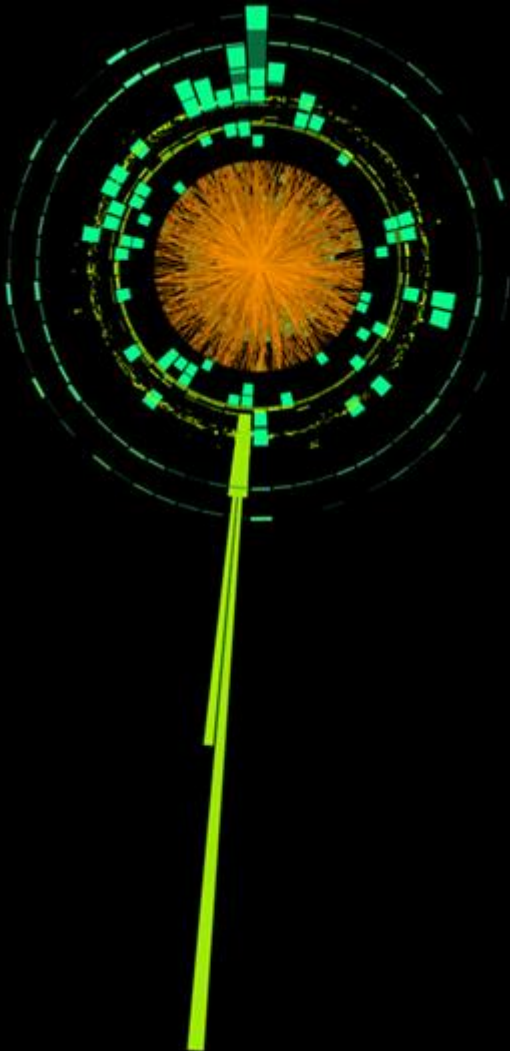
Timothy Rinn

$$p_T^Y = 420.1 \text{ GeV}$$

$$p_T^{\text{Jet}} = 289.7 \text{ GeV}$$

$$\Sigma E_T^{\text{FCal}} = 3.74 \text{ TeV}$$

Jets as probe of QGP:



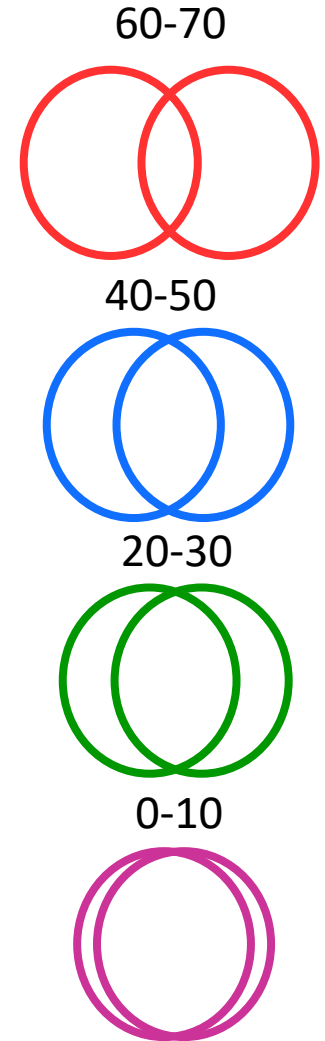
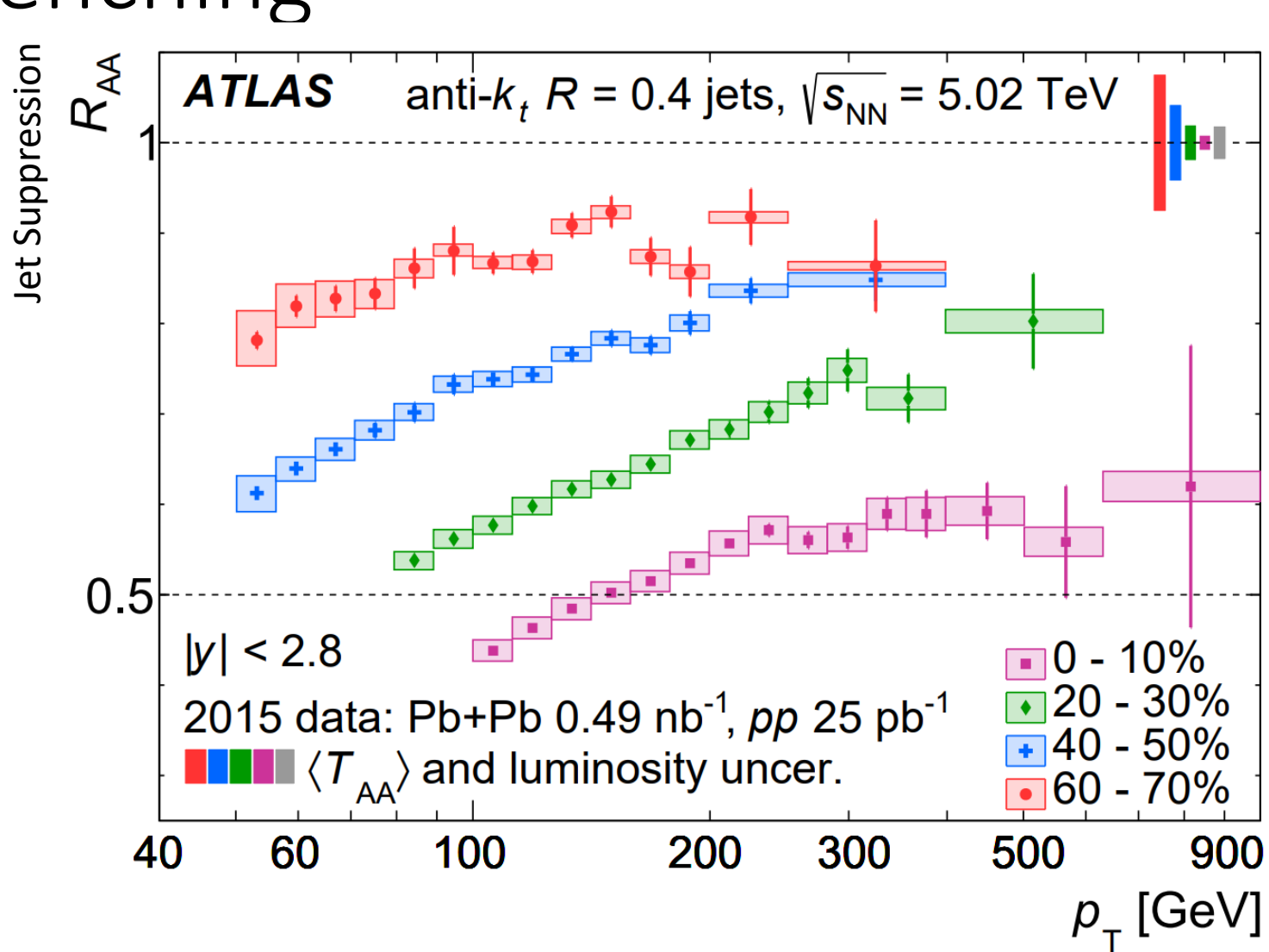
Quarks and Gluons interact with the QGP as they traverse the nuclear medium

- Multiple scatterings with quarks and gluons
- Experience medium induced gluon radiation

Results in energy moved outside of the jet cone

Jets Quenching

$$R_{AA} \equiv \frac{\frac{1}{N_{evnt} \langle T_{AA} \rangle} \frac{dN^{AA}}{dp_T}}{\frac{1}{L_{pp}} \frac{dN^{pp}}{dp_T}}$$



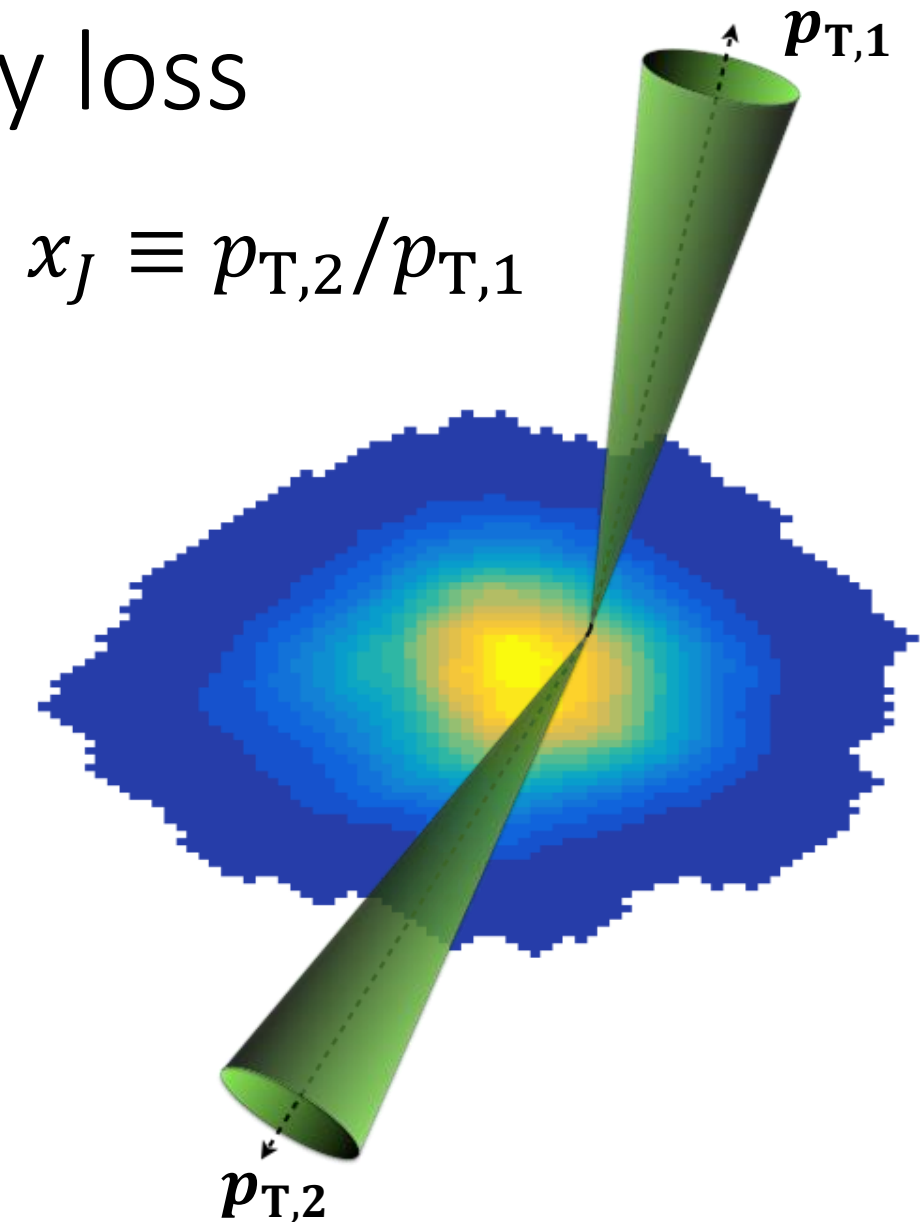
Dijets as probes of energy loss

Back-to-back jet pairs provide access to asymmetric energy loss

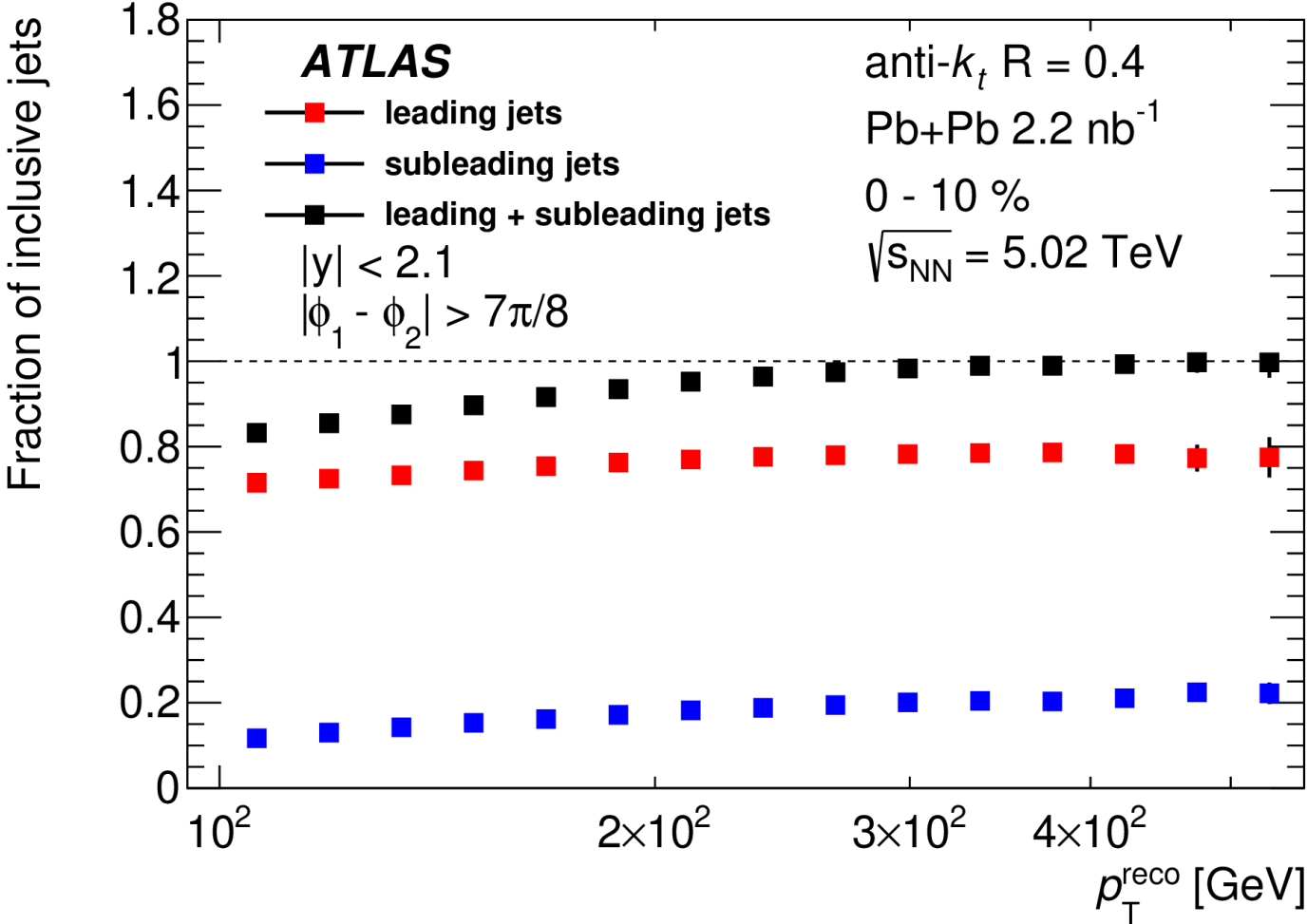
Can provide constraint on the contributions from:

- Path length dependent energy loss
- Energy loss fluctuations

Provide enhanced sensitivity to small amounts of jet quenching



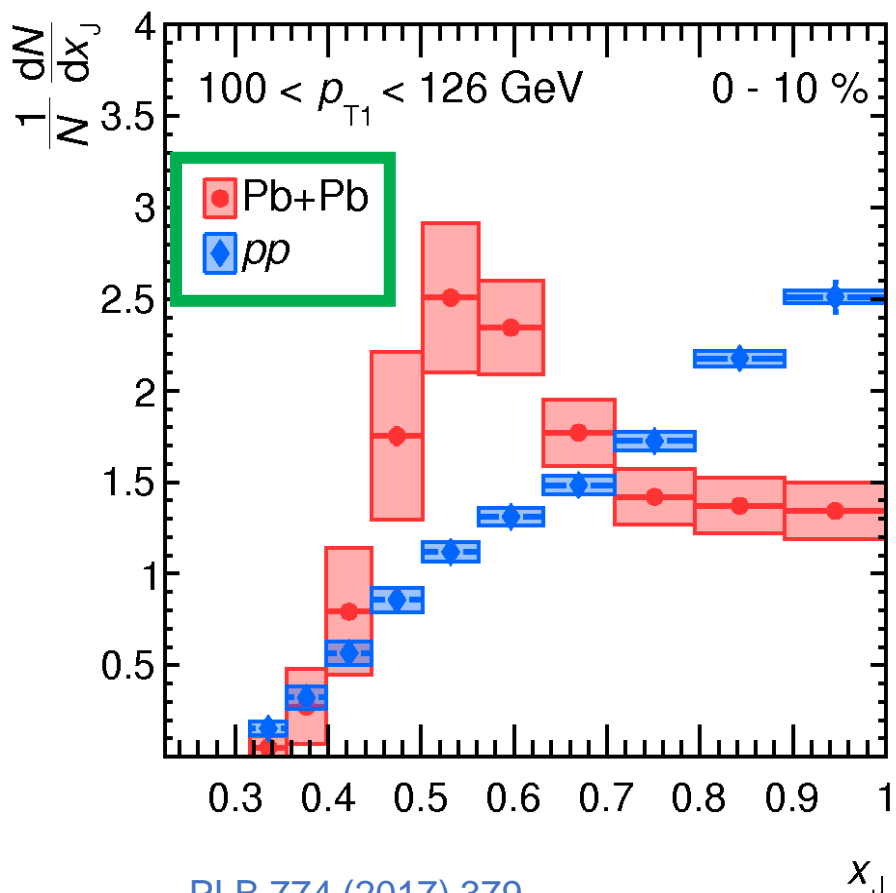
Dijet fraction of inclusive jets



Measured fractions of inclusive jets which are part of the leading **dijet**, the **leading jet** of the dijet, or the **subleading jet** of the dijet

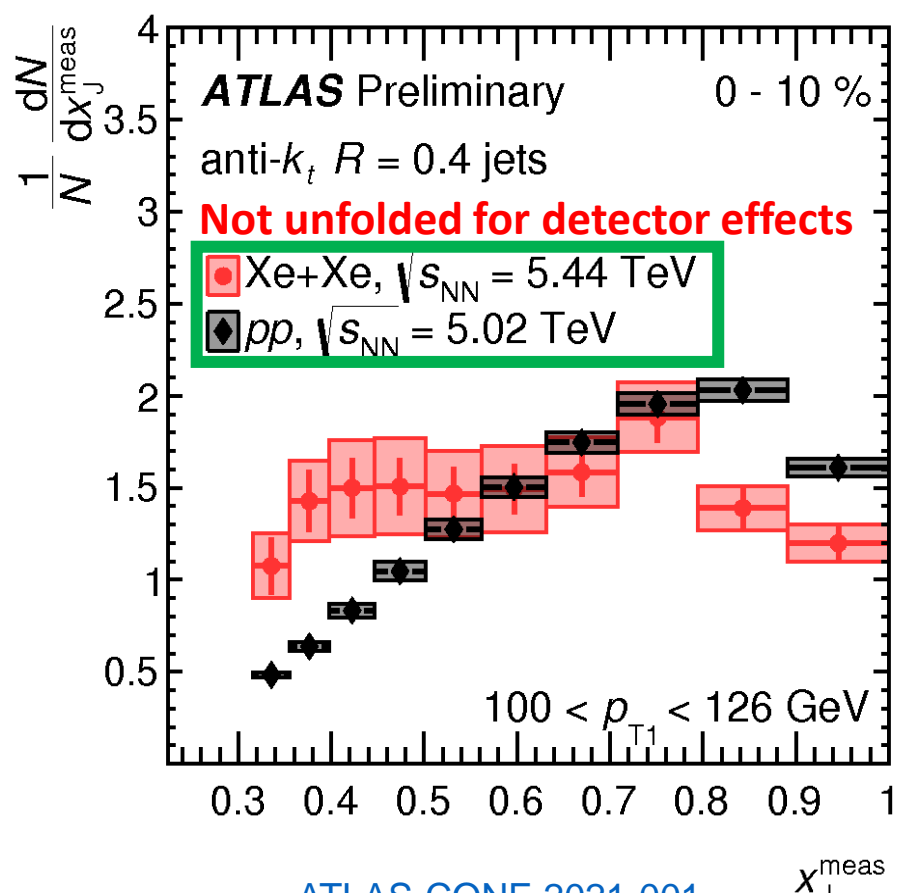
At 100 GeV: 83% of inclusive jets are part of the leading dijet
 ➤ Over 95% for $p_T^{\text{reco}} > 200 \text{ GeV}$

Previous ATLAS results of dijet balance



PLB 774 (2017) 379
(see also: PRL 105(2010) 252303)

4/19/2022



[ATLAS-CONF-2021-001](#)

Timothy Rinn

Modifications of the x_J **shape** are measured in both Pb+Pb and Xe+Xe

In central Pb+Pb a peak structure is observed at intermediate x_J

➤ A persistent challenge for the theory community

Dijet analysis overview:

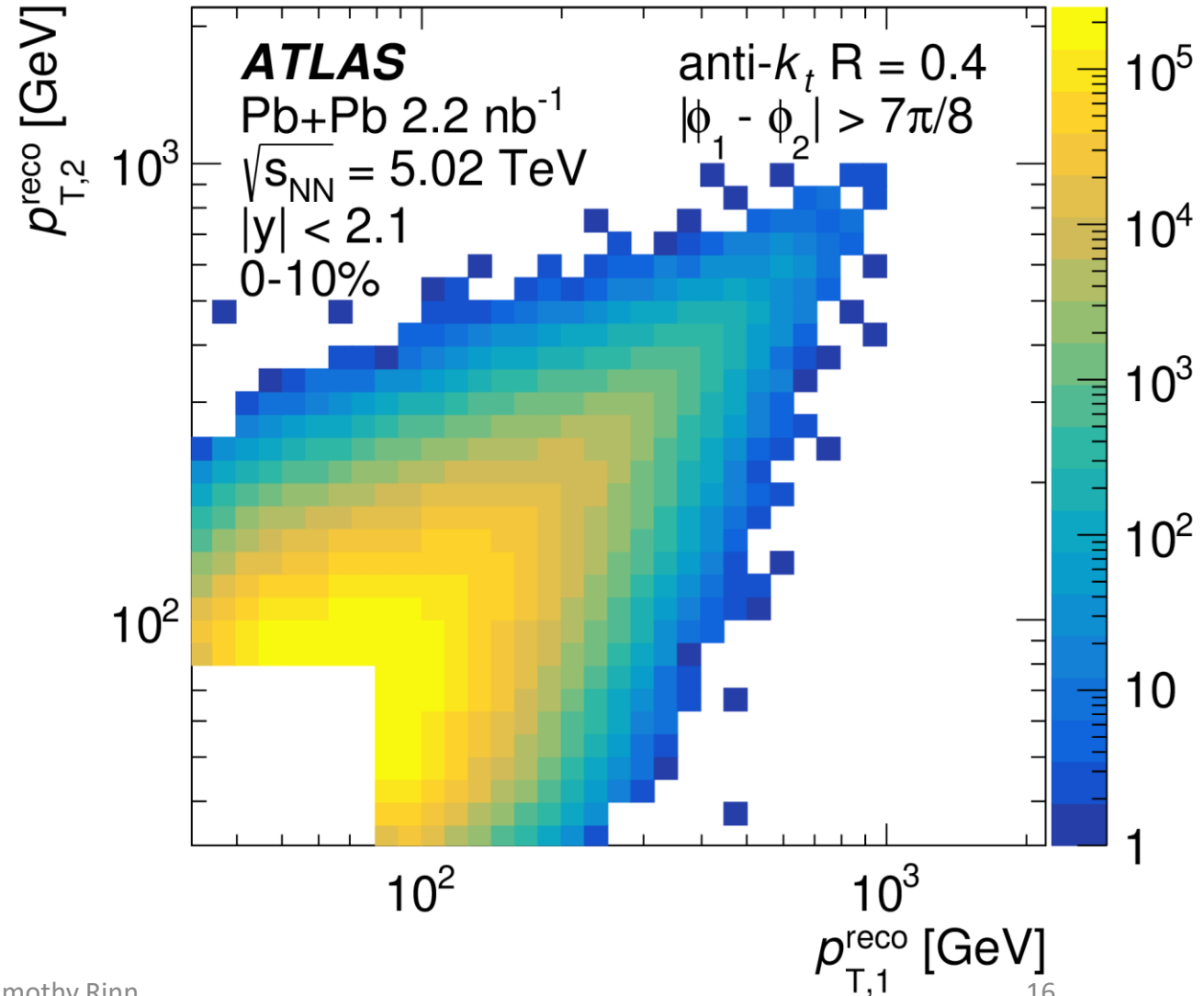
Two-dimensional $(p_{T,1}, p_{T,2})$ distributions are measured for the leading dijet pair

- $\Delta\phi_{1,2} > \frac{7\pi}{8}$
- $|\eta| < 2.1$

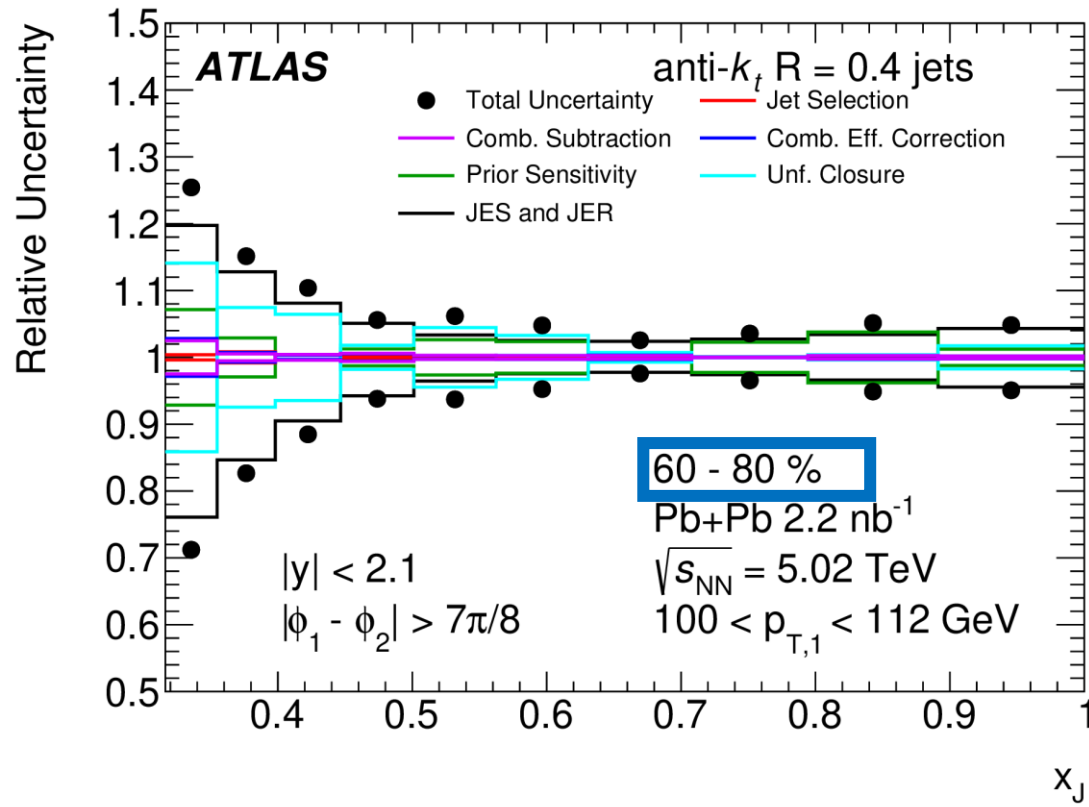
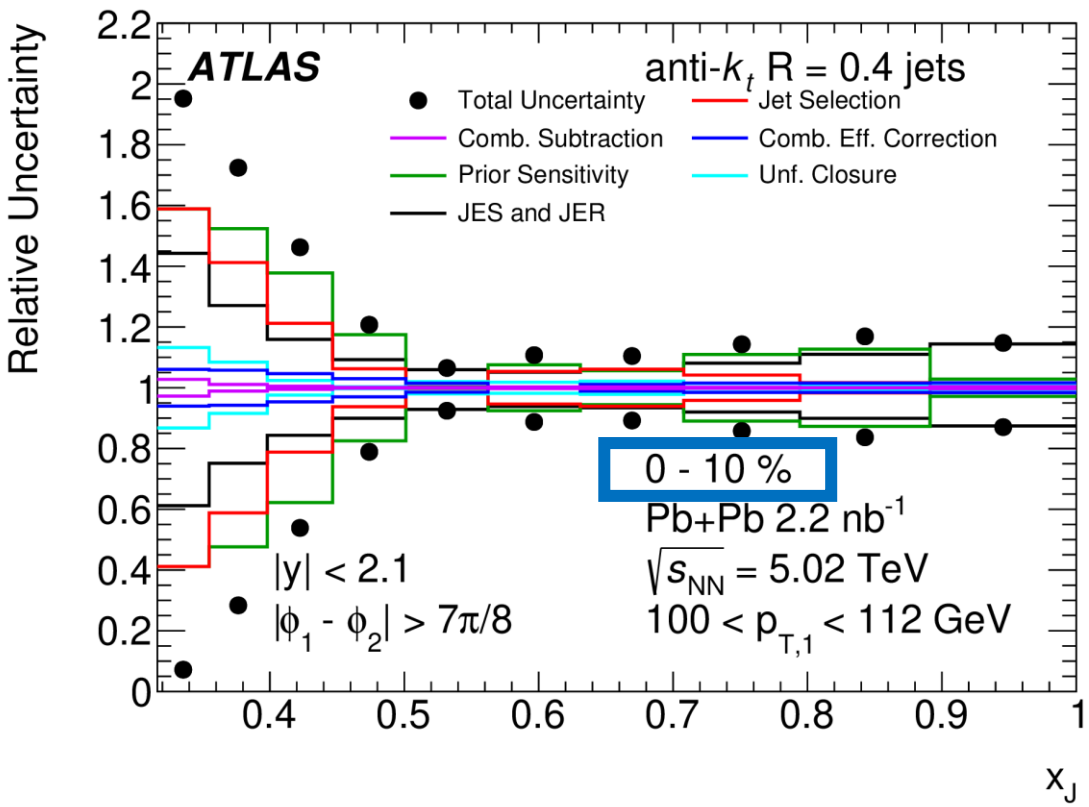
Corrected for combinatoric dijets using a $\Delta\phi_{1,2}$ sideband

Unfolded for detector effects using 2D Bayesian unfolding

Unfolded $\frac{dN_{pair}}{dp_{T,1}dp_{T,2}}$ distribution projected across selections of $p_{T,1}$ to extract $\frac{dN}{dx_J}$ distributions



Uncertainties on per dijet pair x_J distributions



In central events the uncertainties are driven by unfolding

In peripheral events the uncertainty from the jet energy scale and resolution are dominant

Dijet x_J observables

Per dijet pair normalized x_J distributions: $\frac{1}{N_{pair}} \frac{dN_{pair}}{dx_J}$

- Enables direct comparison of the x_J shape across centrality in Pb+Pb and in pp

Absolutely normalized x_J distributions: $\frac{1}{N_{evt} \langle T_{AA} \rangle} \frac{dN_{pair}}{dx_J}$

- Enables evaluation of the dijet per event yields as a function of x_J
- Provides insight into the dynamics of dijet energy loss

Never Before Measured

Dijet x_J observables

Per dijet pair normalized x_J distributions: $\frac{1}{N_{pair}} \frac{dN_{pair}}{dx_J}$

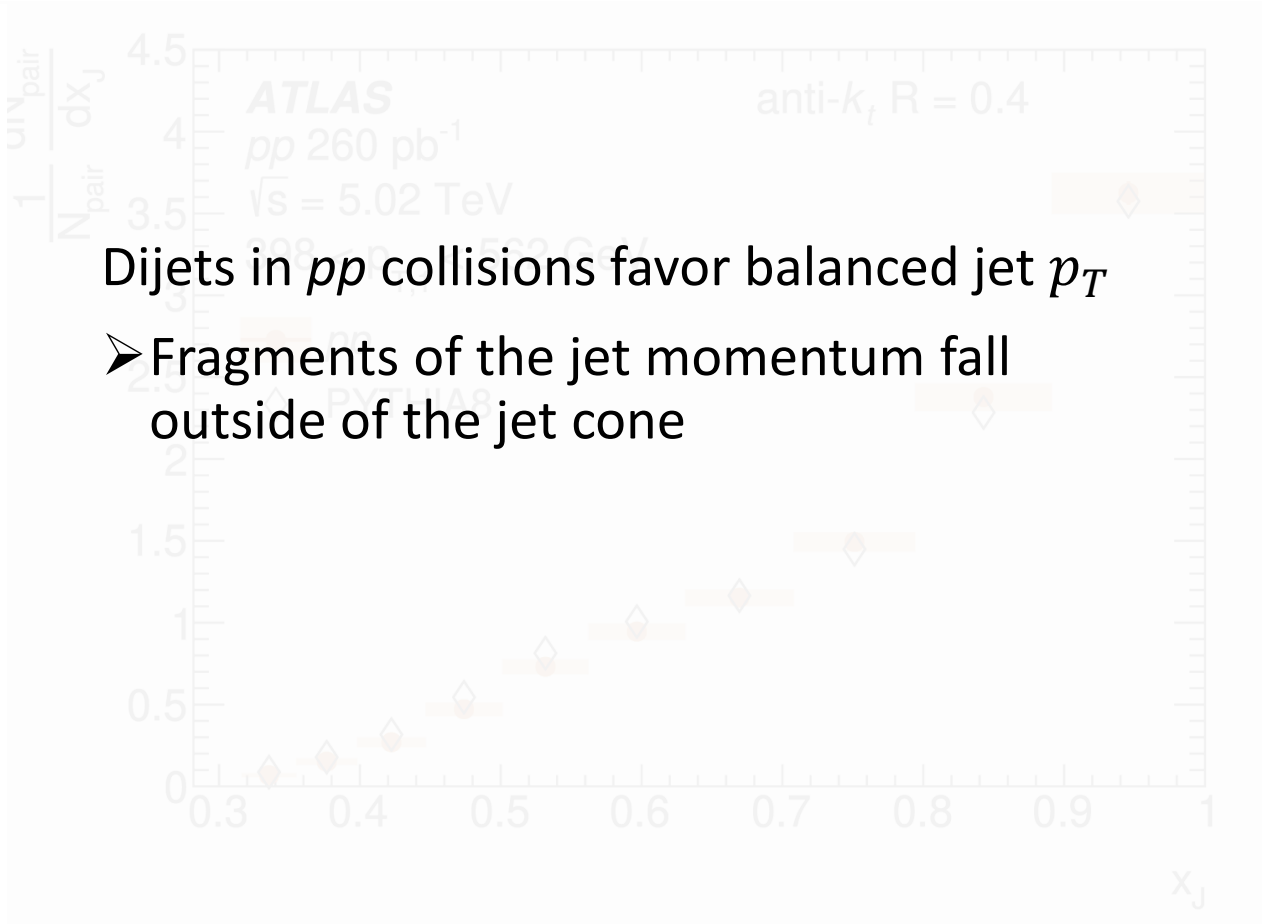
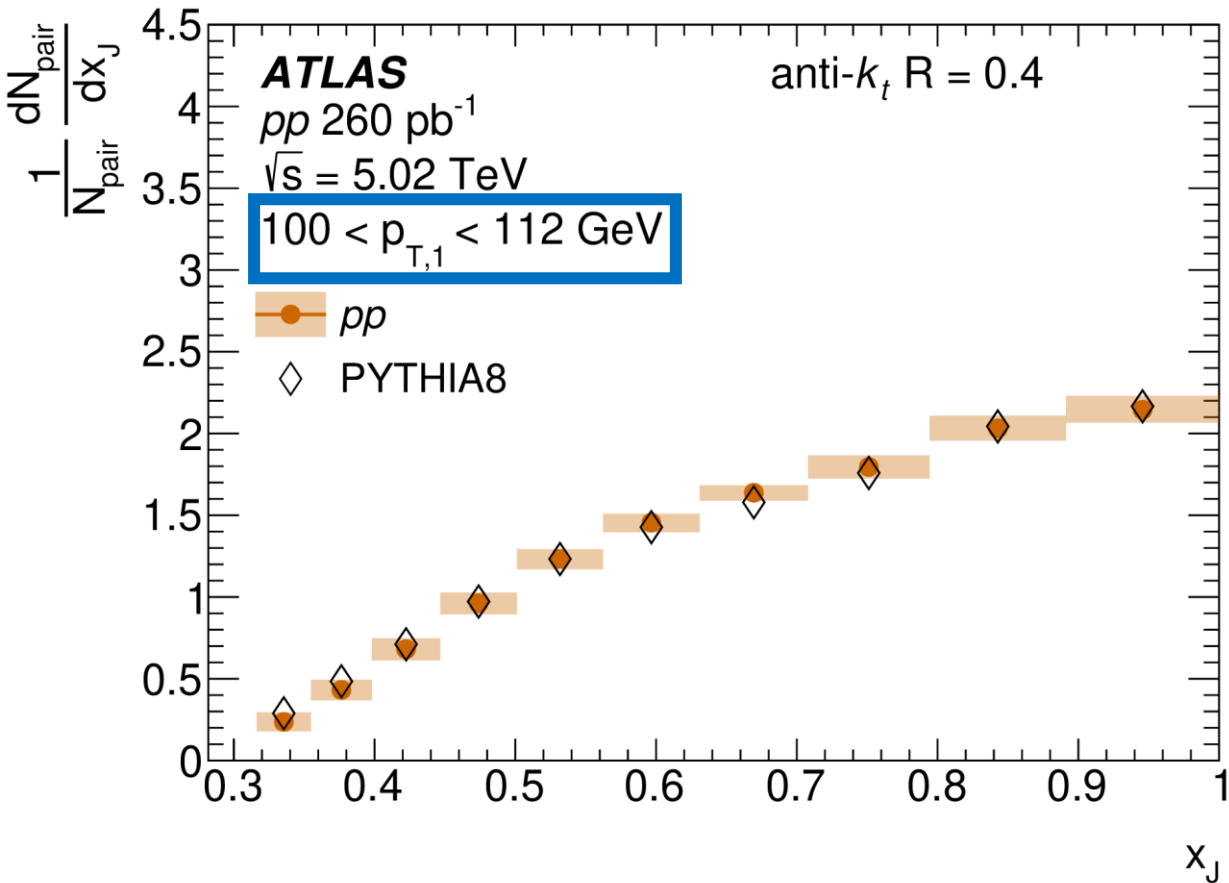
- Enables direct comparison of the x_J shape across centrality in Pb+Pb and in pp

Absolutely normalized x_J distributions: $\frac{1}{N_{evt} \langle T_{AA} \rangle} \frac{dN_{pair}}{dx_J}$

- Enables evaluation of the dijet per event yields as a function of x_J
- Provides insight into the dynamics of dijet energy loss

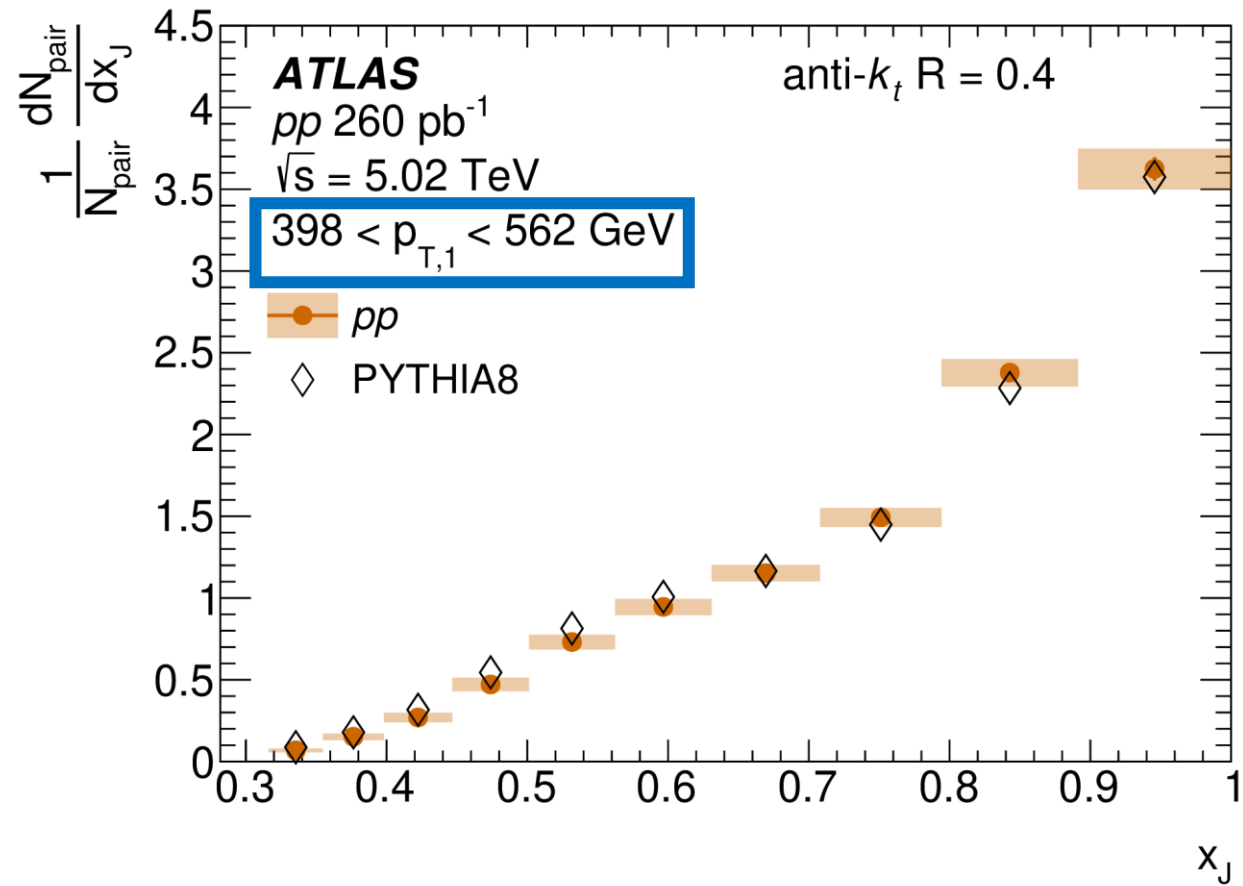
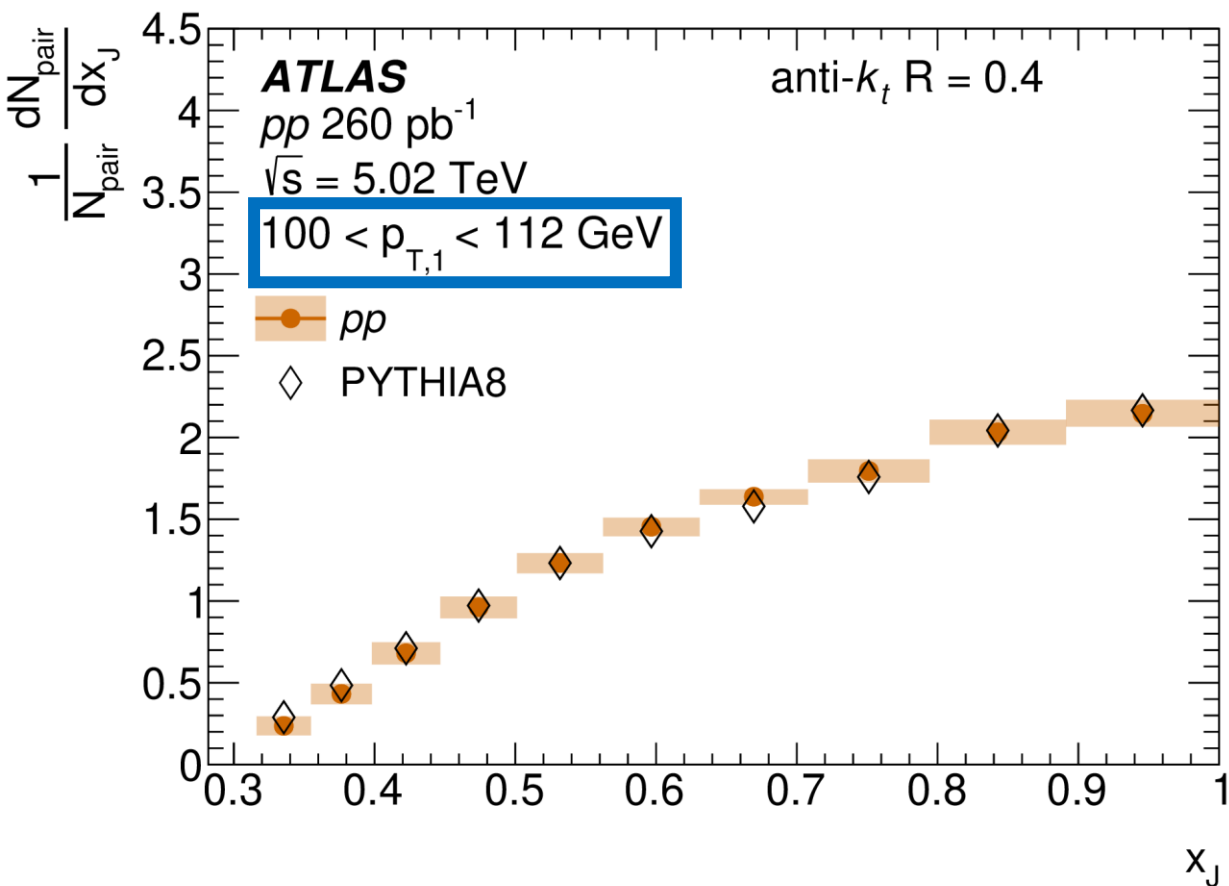
Never Before Measured

$\frac{1}{N_{pair}} \frac{dN_{pair}}{dx_J}$ pp results



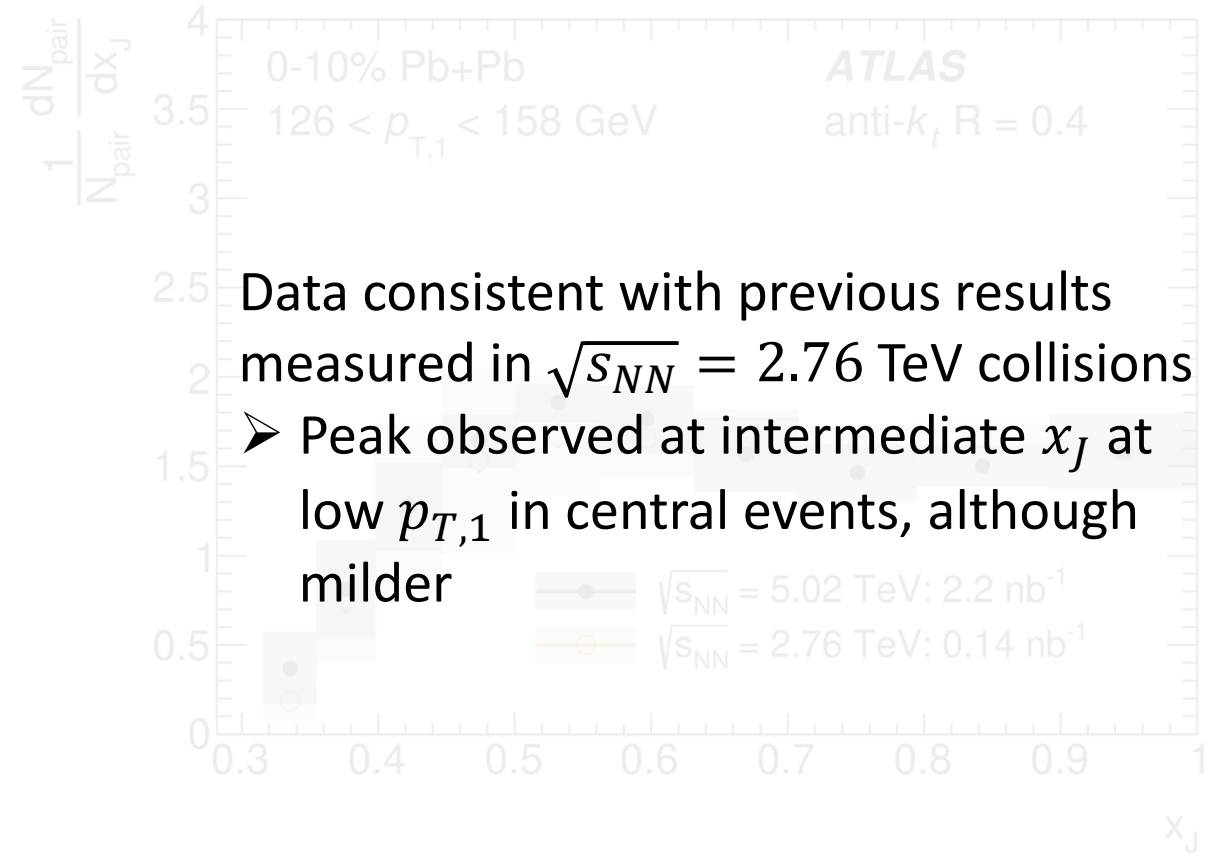
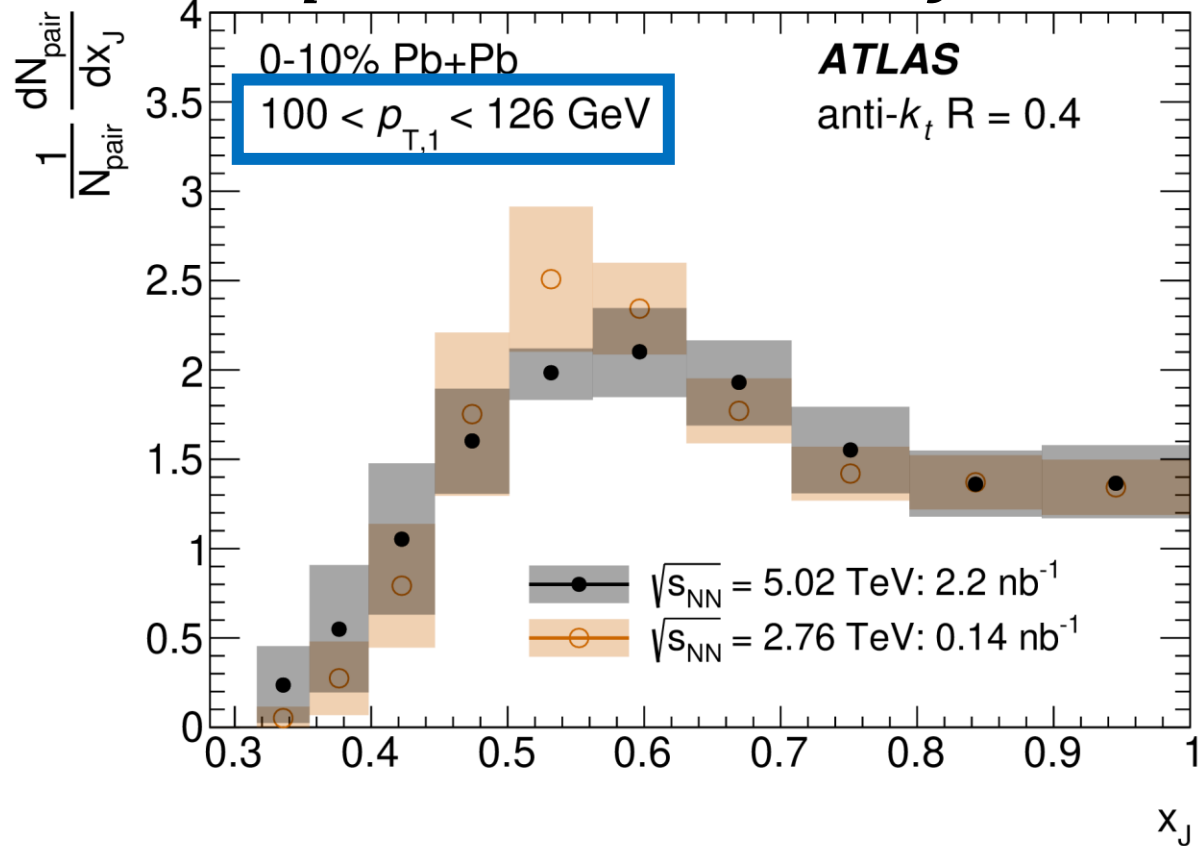
- Dijets in pp collisions favor balanced jet p_T
- Fragments of the jet momentum fall outside of the jet cone

$1/N_{pair} \frac{dN_{pair}}{dx_J}$ pp results

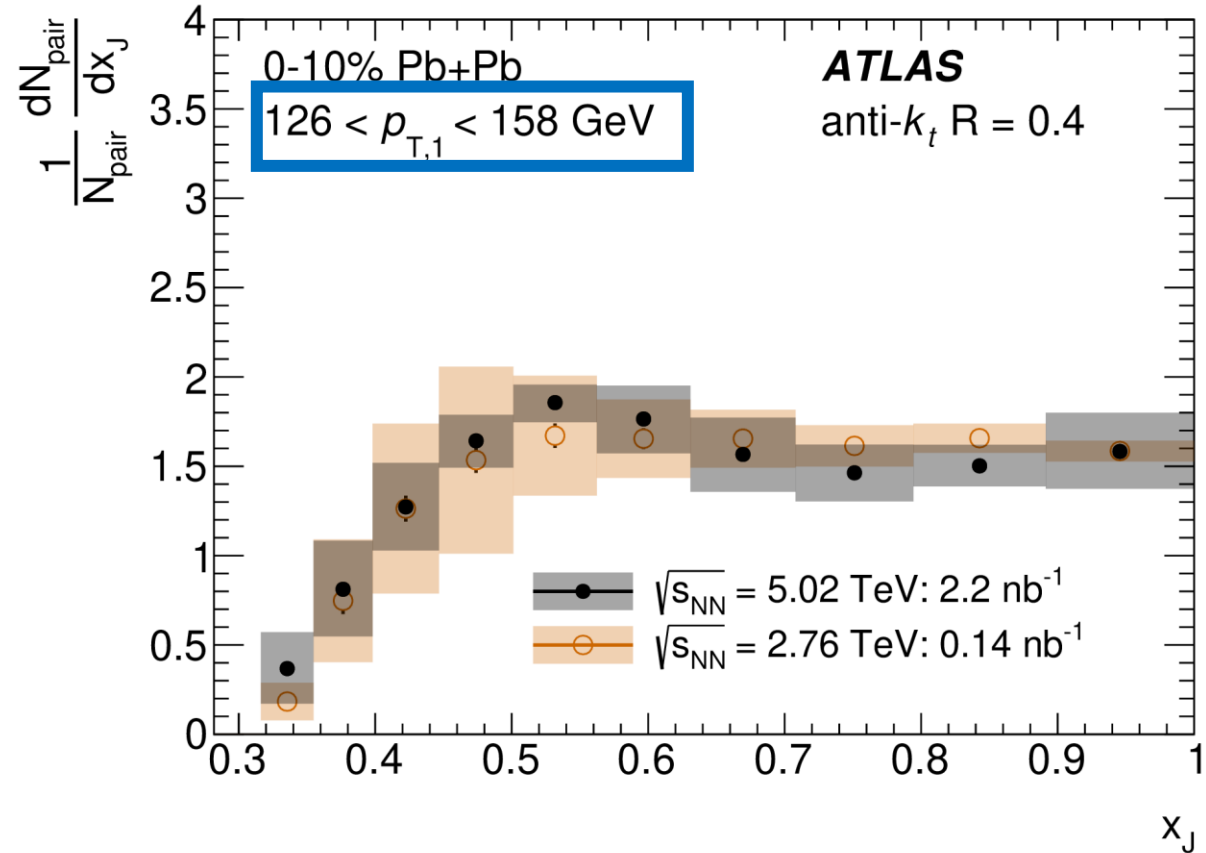
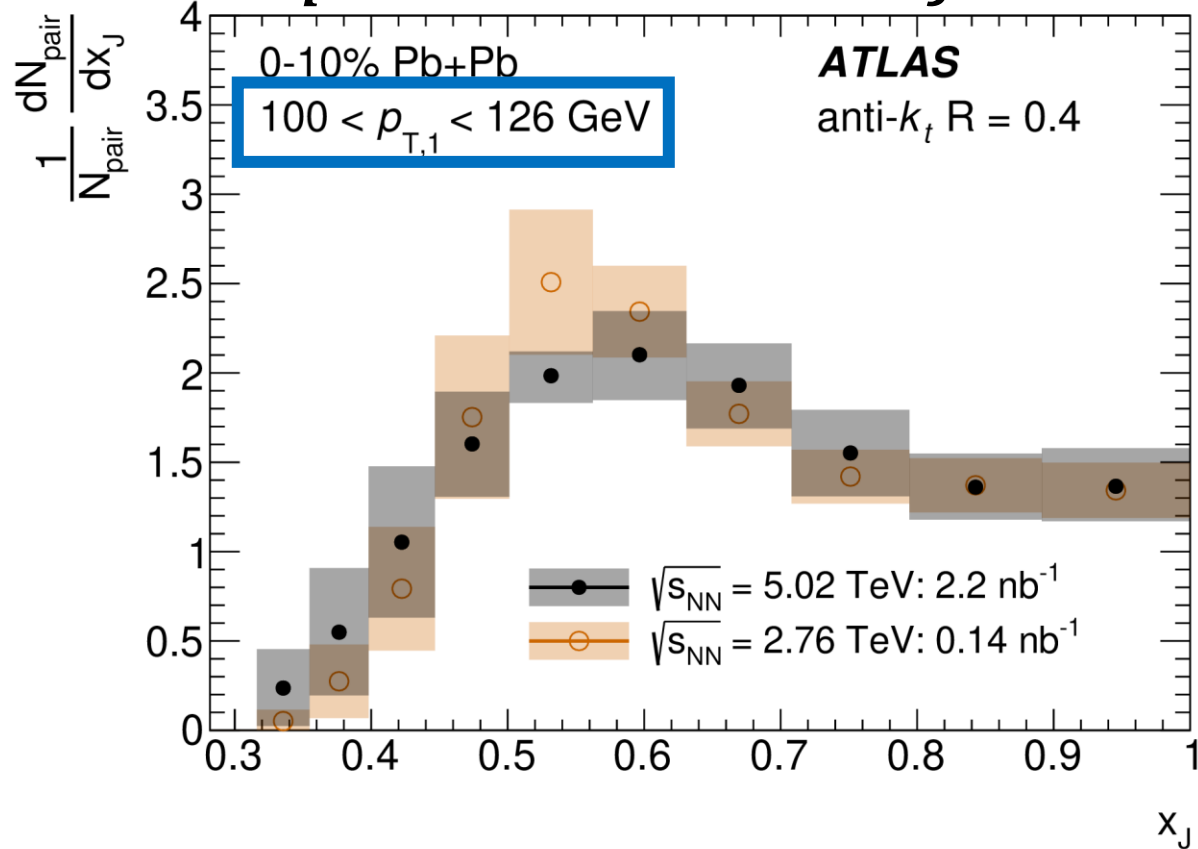


Higher p_T jets \rightarrow more collimated \rightarrow more balanced

$1/N_{pair} \frac{dN_{pair}}{dx_J}$ distributions

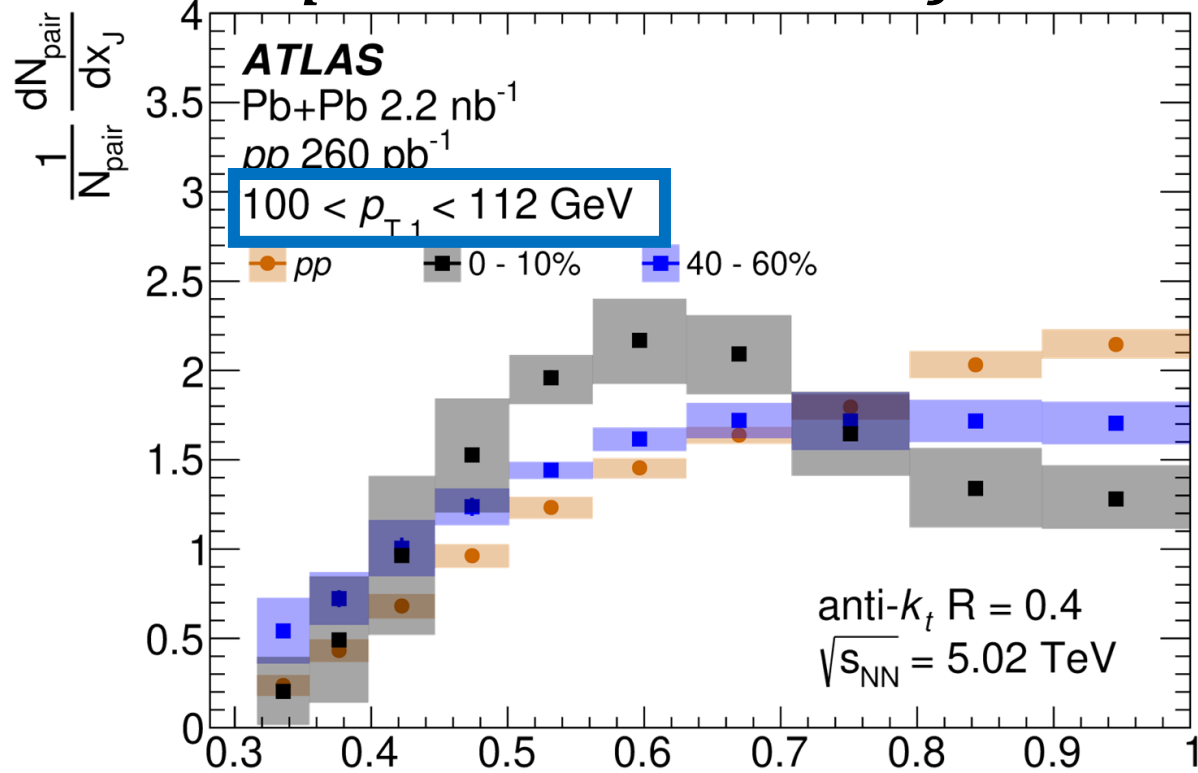


$1/N_{pair} \frac{dN_{pair}}{dx_J}$ distributions

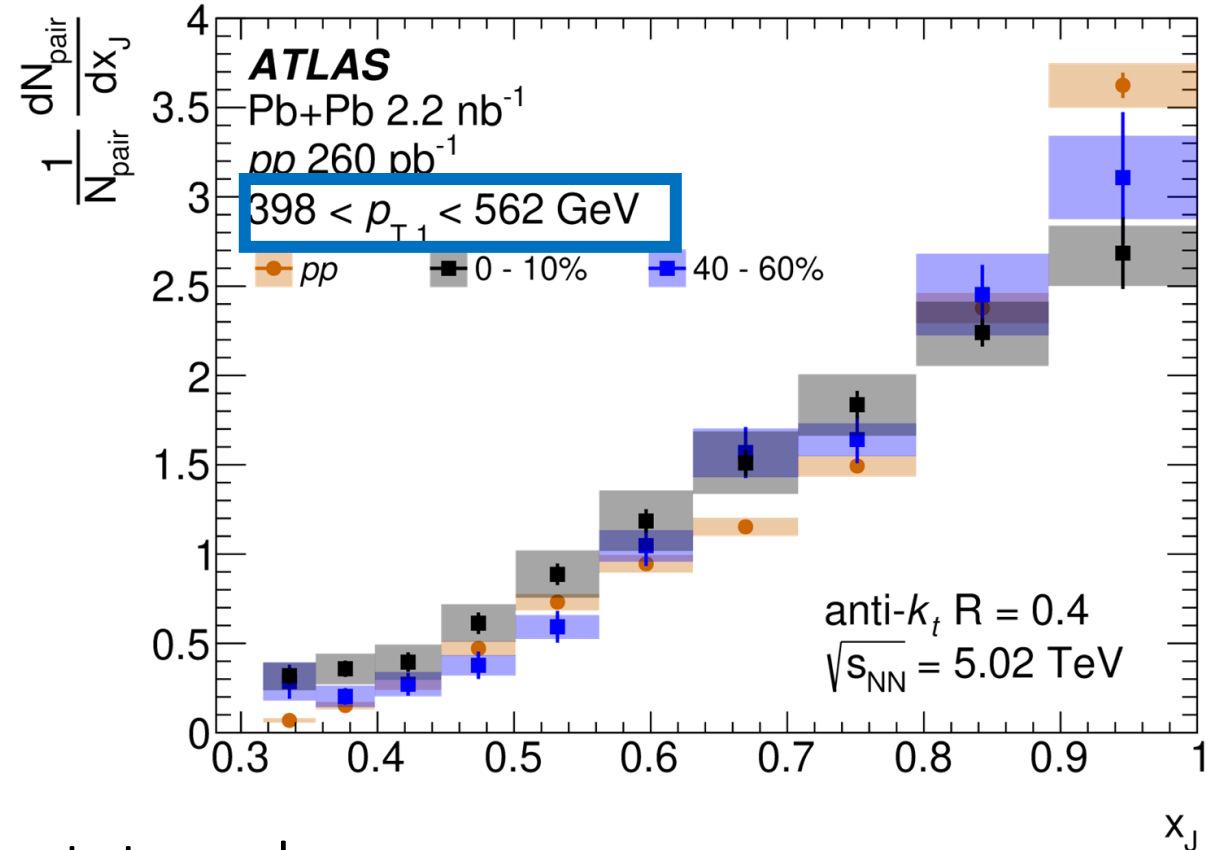


Both results observe significant flattening of the peak structure with increasing leading jet p_T

$1/N_{pair} \frac{dN_{pair}}{dx_J}$ distributions

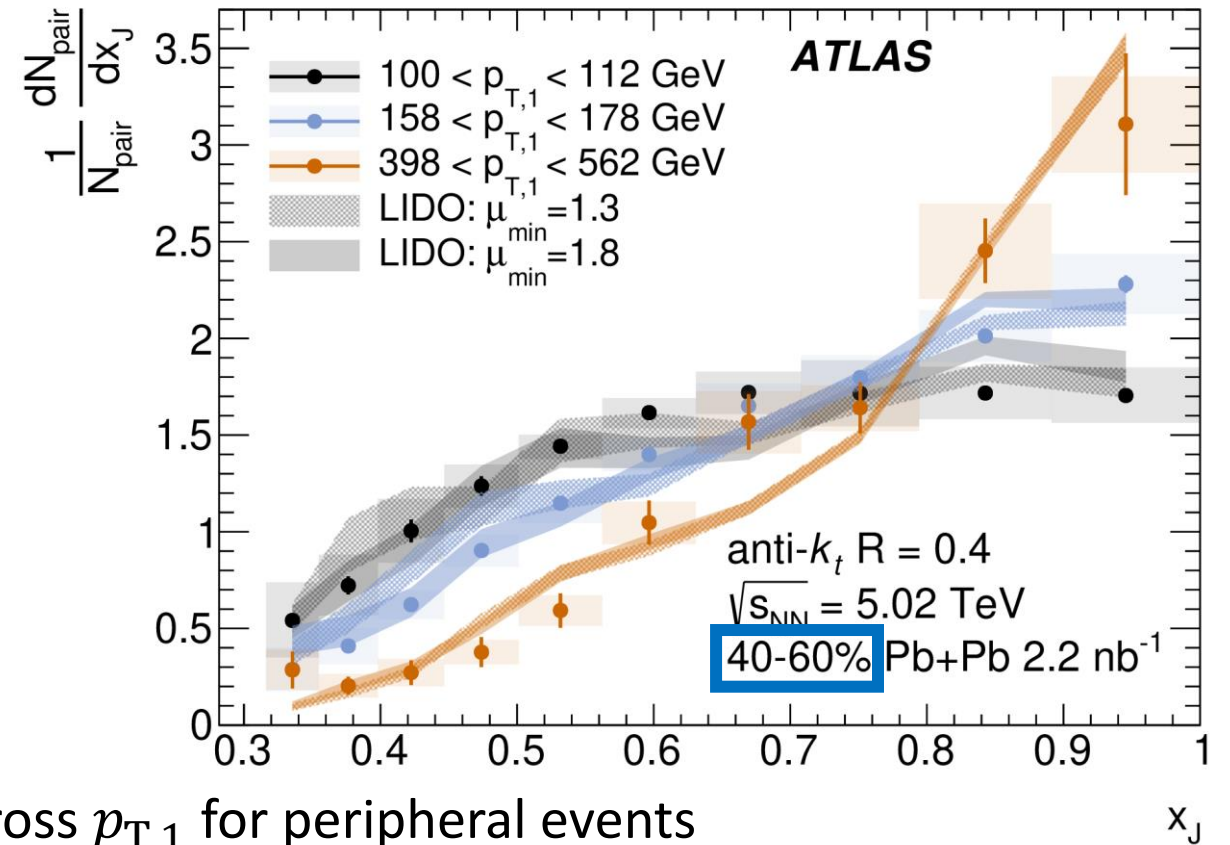
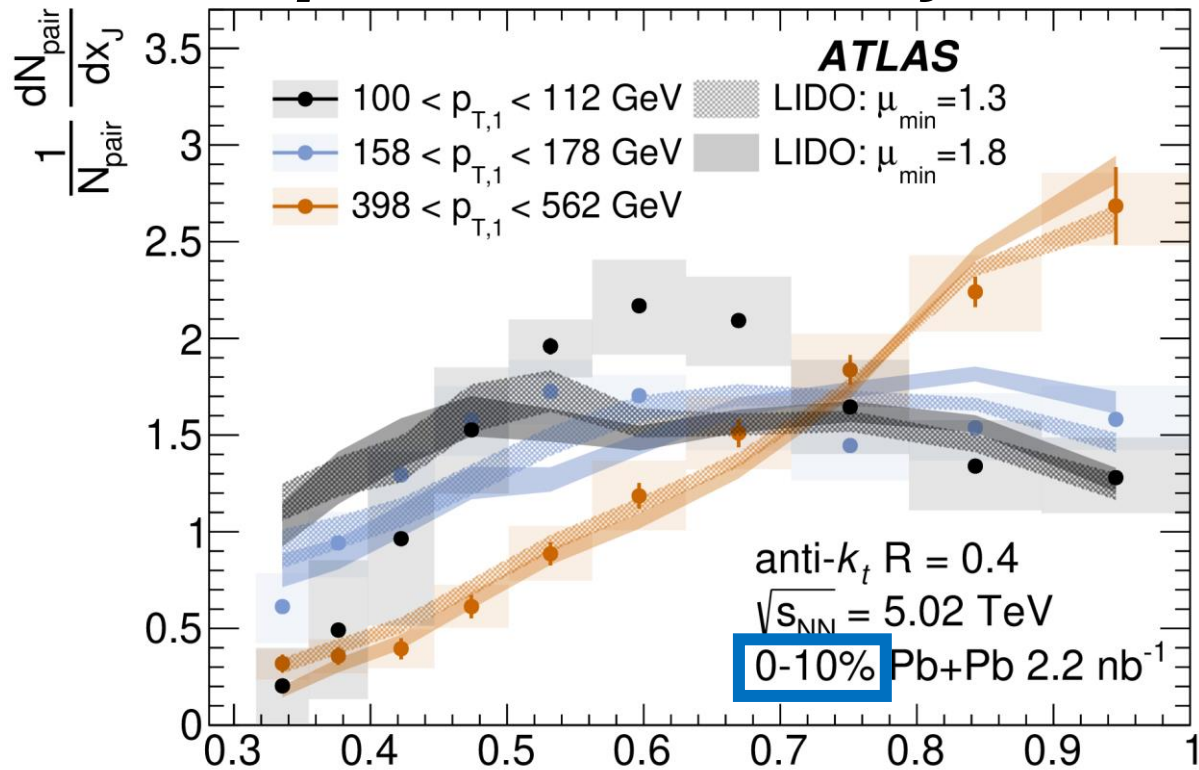


Smooth evolution from central Pb+Pb events towards pp



Significant modifications from pp collisions observed even at the highest $p_{T,1}$

$\frac{1}{N_{pair}} \frac{dN_{pair}}{dx_J}$: Comparison with theory



LIDO calculations well predicts the behavior across $p_{T,1}$ for peripheral events

➤ Reproduces the x_J shape for intermediate and high $p_{T,1}$ in central events

LIDO does not reproduce the peak observed at intermediate x_J at low $p_{T,1}$

Dijet x_J observables

Per dijet pair normalized x_J distributions: $\frac{1}{N_{pair}} \frac{dN_{pair}}{dx_J}$

- Enables direct comparison of the x_J shape across centrality in Pb+Pb and in pp

Absolutely normalized x_J distributions: $\frac{1}{N_{evt} \langle T_{AA} \rangle} \frac{dN_{pair}}{dx_J}$

- Enables evaluation of the dijet per event yields as a function of x_J
- Provides insight into the dynamics of dijet energy loss

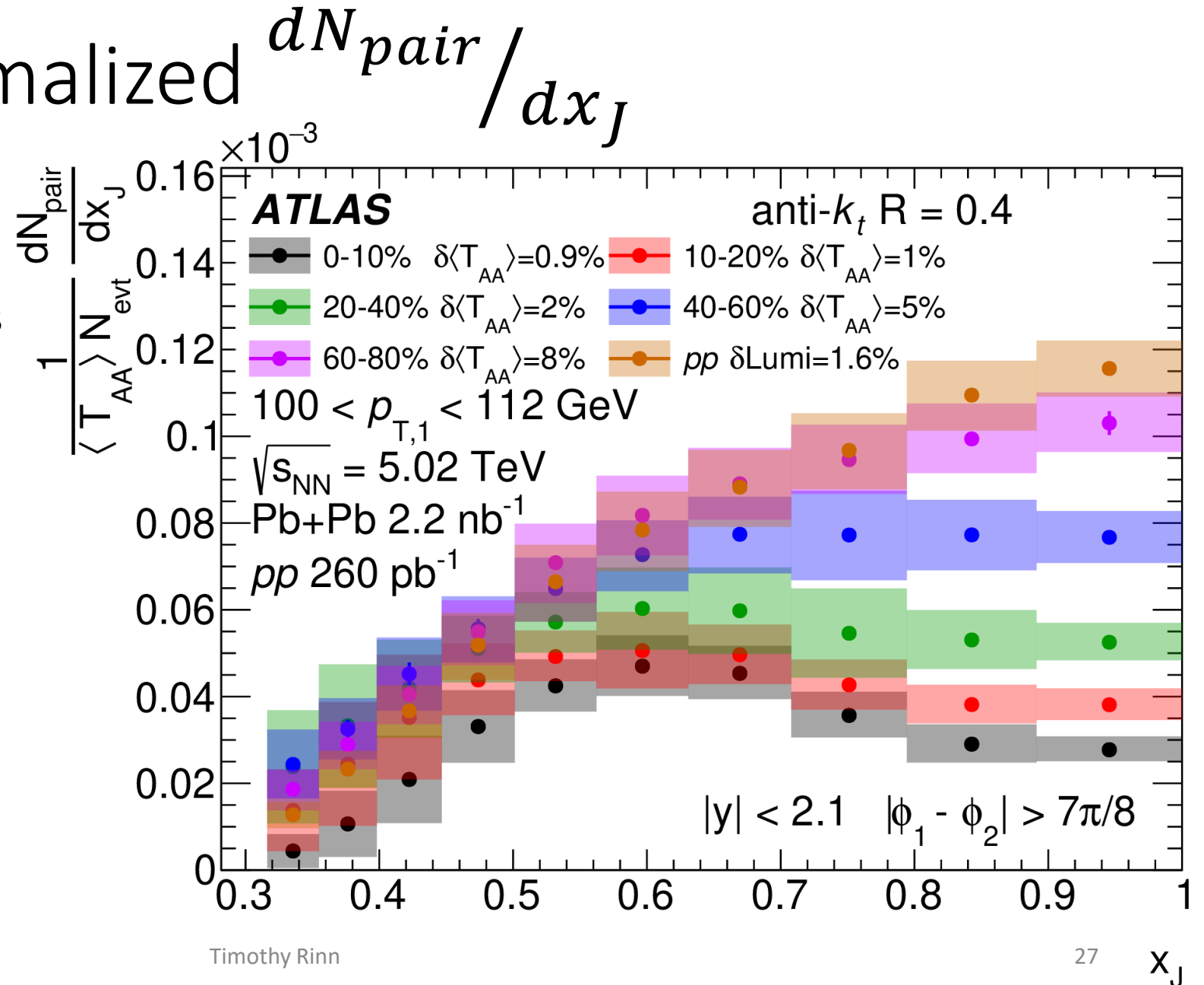
Never Before Measured

Absolutely normalized dN_{pair}/dx_J

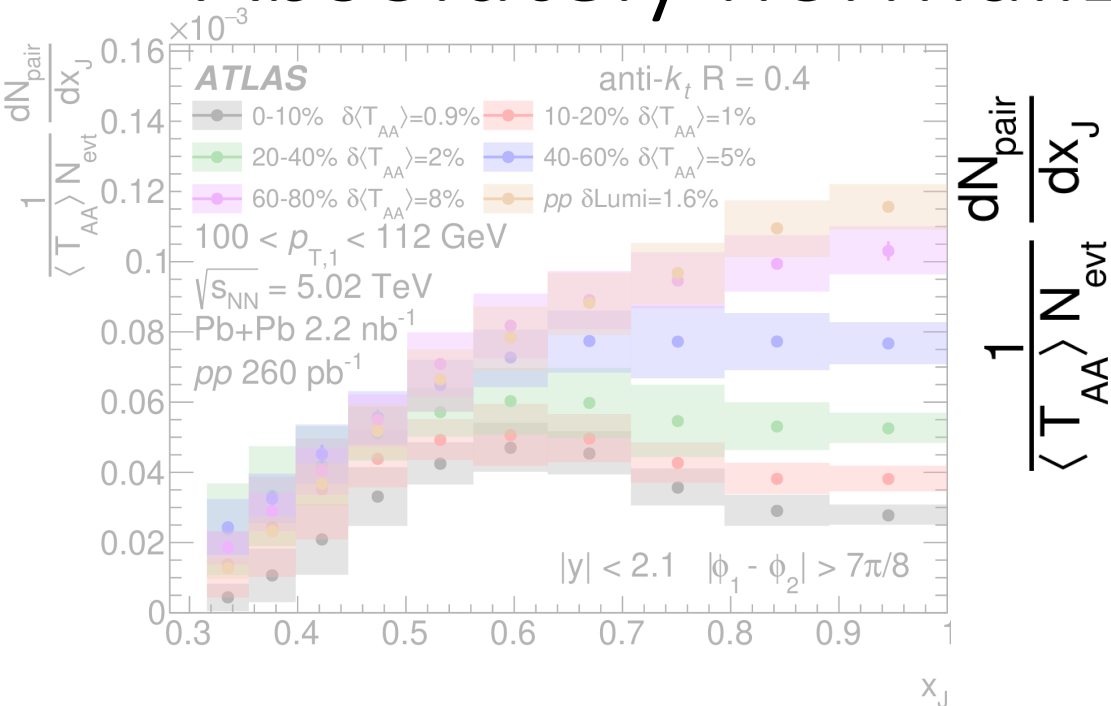
Using a $\frac{1}{\langle T_{AA} \rangle N_{evt}}$ normalization enables the study of dijet yields as a function of x_J

The peak structure observed at intermediate x_J stems from the favorable suppression of symmetric dijets

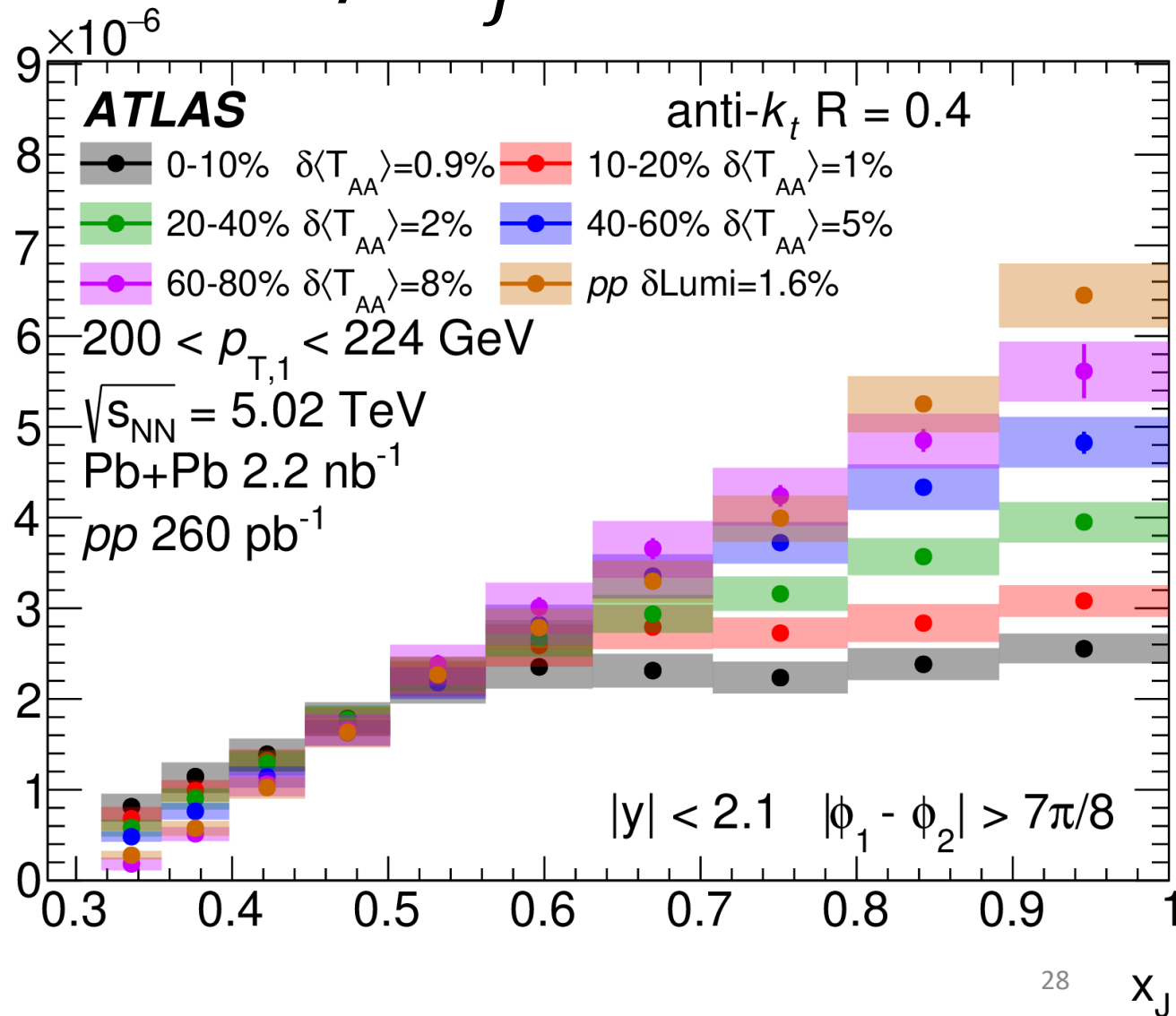
- No evidence for enhancement over pp of intermediate x_J



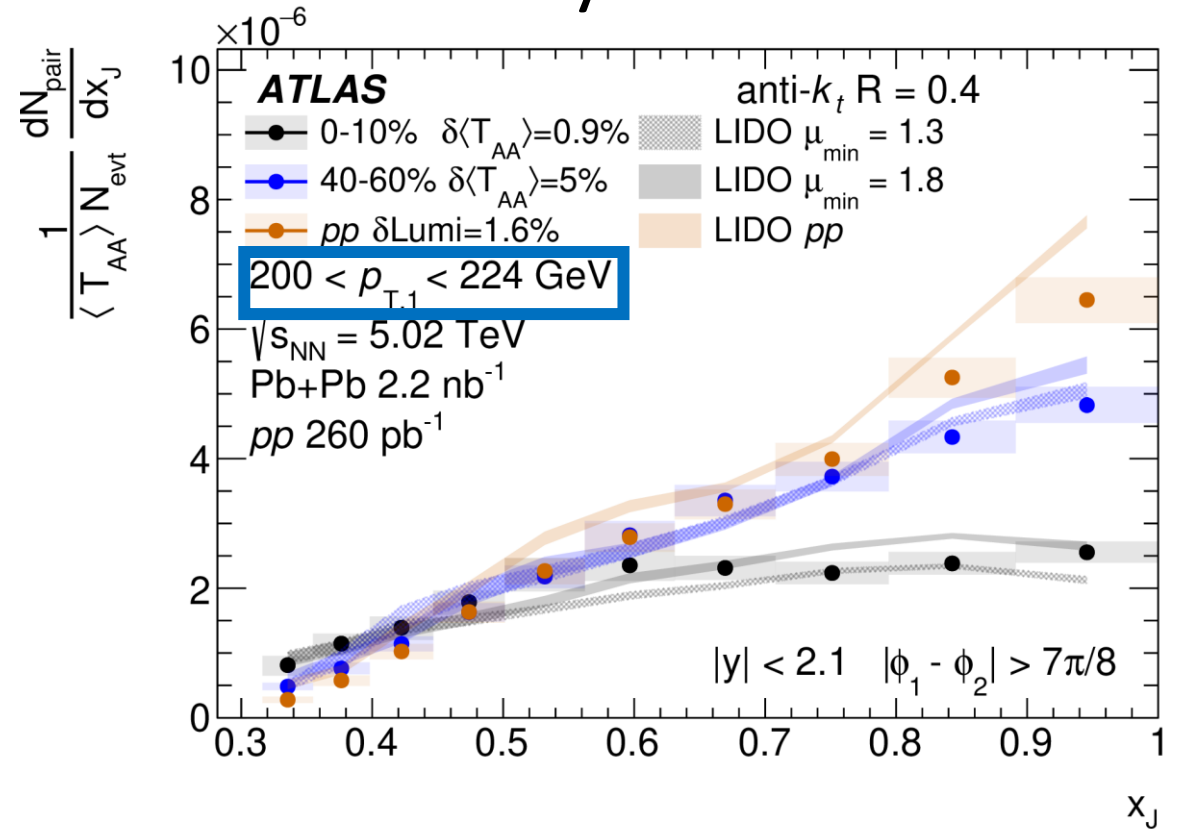
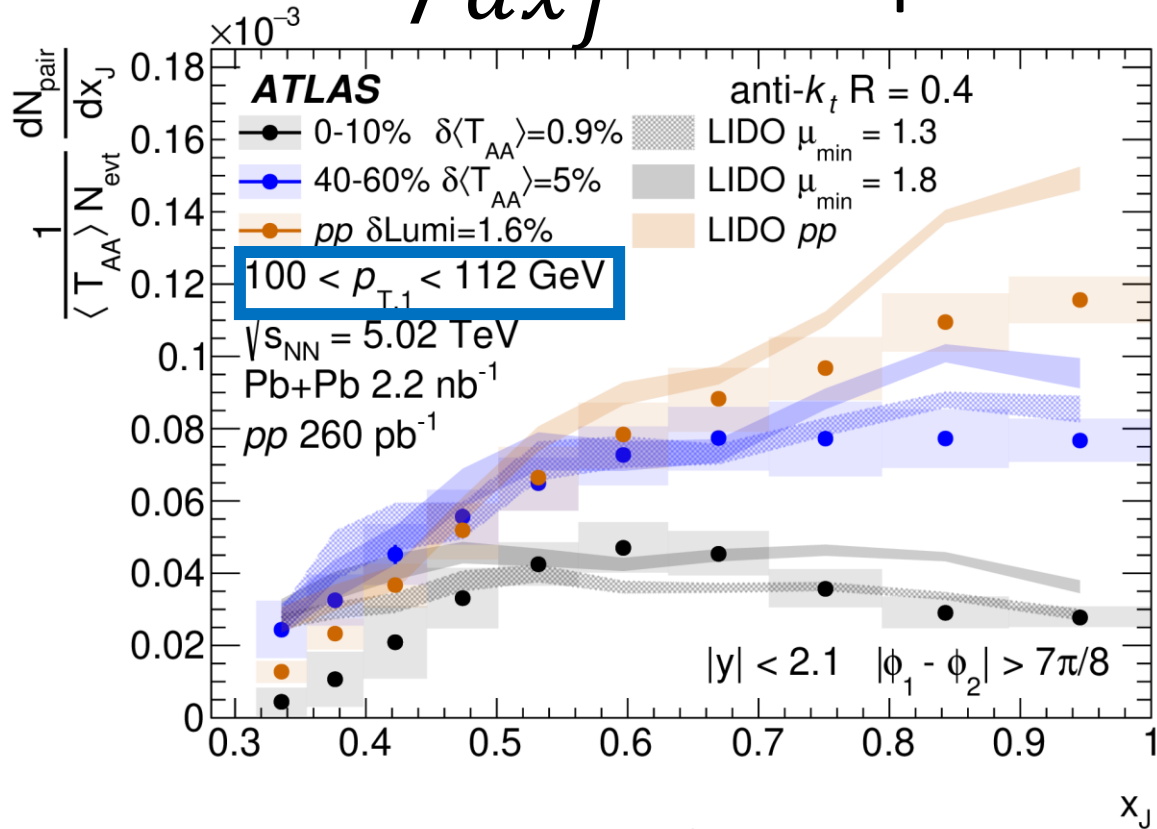
Absolutely normalized dN_{pair}/dx_J



The systematic suppression of symmetric dijets persists with increasing $p_{T,1}$



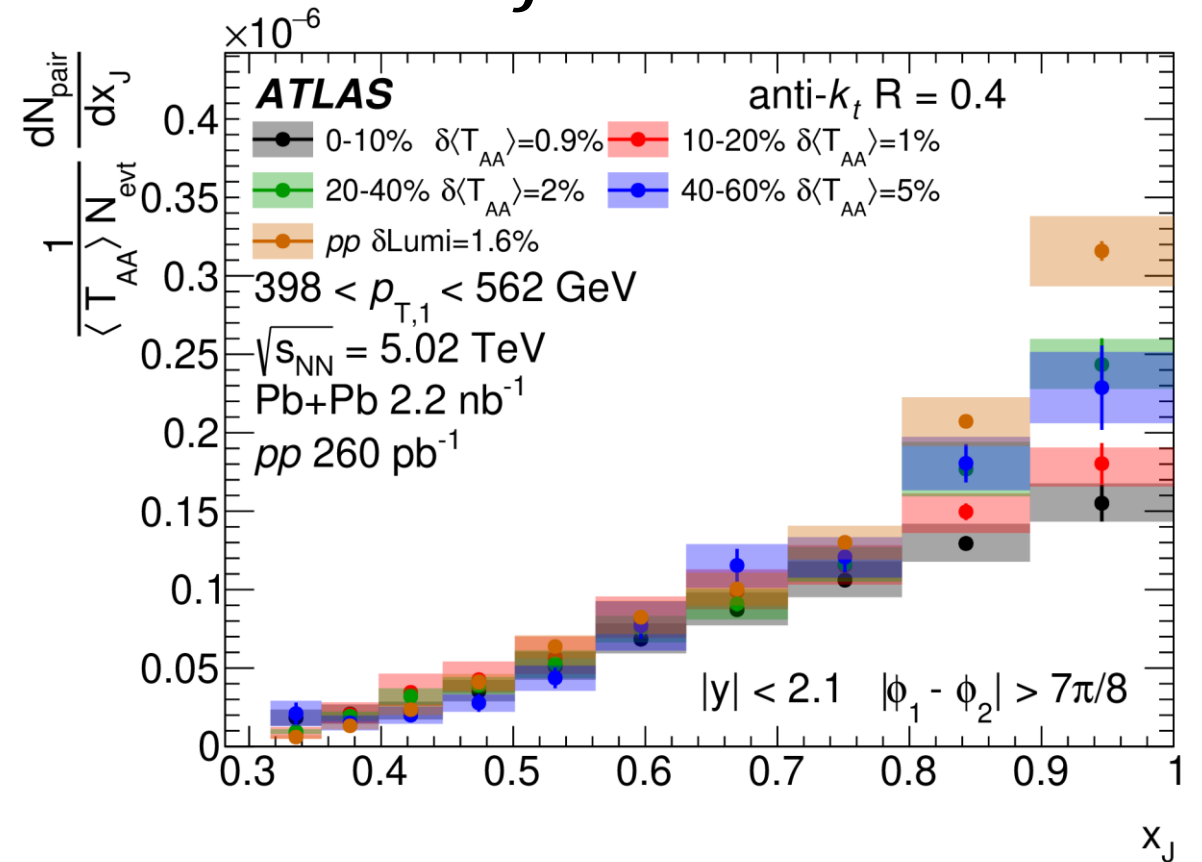
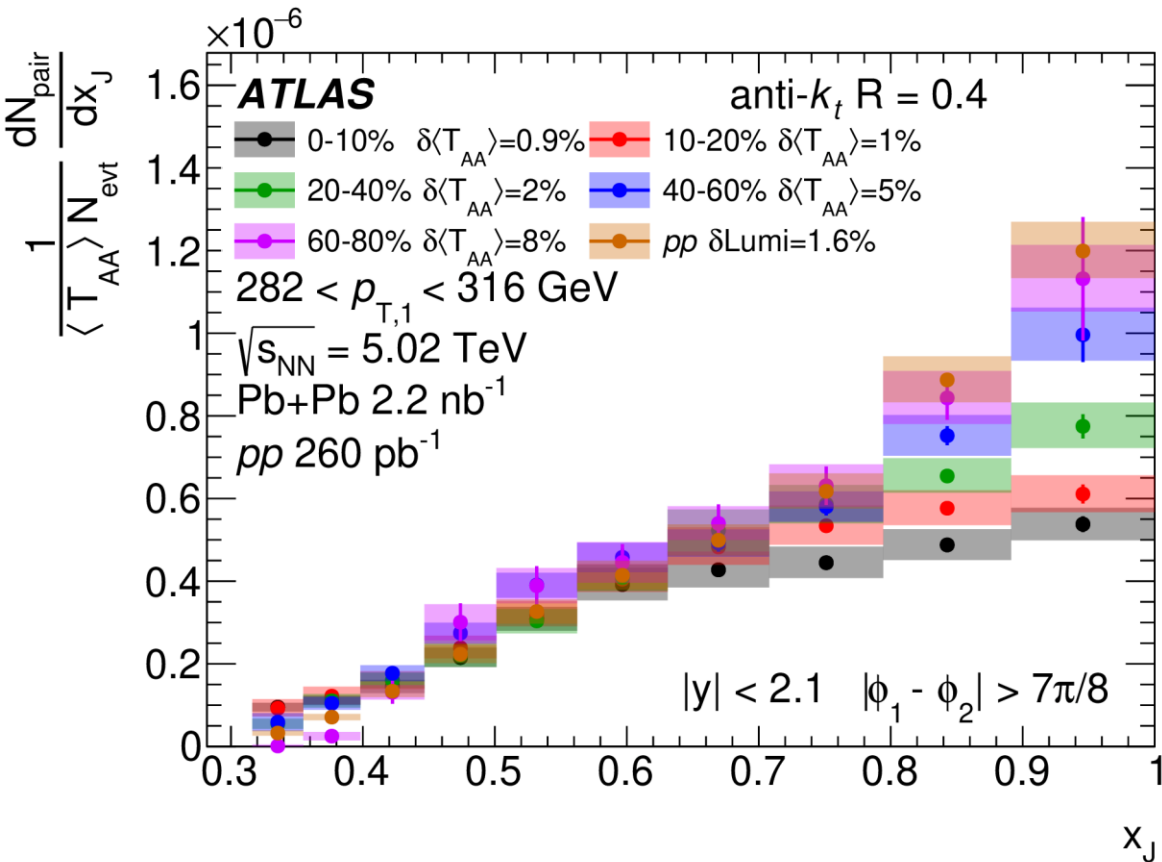
dN_{pair}/dx_J : Comparison with theory



The absolute yield of dijet pairs at low $p_{T,1}$ are overestimated by the Pythia8 A14 tune with CTEQL1 PDF used in LIDO

LIDO qualitatively predicts the depletion of symmetric dijets observed across $p_{T,1}$

Absolutely normalized dN_{pair}/dx_J



Significant suppression of symmetric dijets measured at the highest $p_{T,1}$


Dijet nuclear modification factor: R_{AA}^{pair}

$$R_{AA}^{pair}(\mathbf{p}_{T,1}) = \frac{\frac{1}{\langle T_{AA} \rangle N_{evt}^{AA}} \int_{0.32 \times \mathbf{p}_{T,1}}^{\mathbf{p}_{T,1}} \frac{d^2 N_{pair}^{AA}}{dp_{T,1} dp_{T,2}} d\mathbf{p}_{T,2}}{\frac{1}{L_{pp}} \int_{0.32 \times \mathbf{p}_{T,1}}^{\mathbf{p}_{T,1}} \frac{d^2 N_{pair}^{pp}}{dp_{T,1} dp_{T,2}} d\mathbf{p}_{T,2}}$$

$R_{AA}^{pair}(\mathbf{p}_{T,1})$ quantifies the suppression of the **leading jet** in a dijet

$$R_{AA}^{pair}(\mathbf{p}_{T,2}) = \frac{\frac{1}{\langle T_{AA} \rangle N_{evt}^{AA}} \int_{\mathbf{p}_{T,2}}^{\mathbf{p}_{T,2}/0.32} \frac{d^2 N_{pair}^{AA}}{dp_{T,1} dp_{T,2}} d\mathbf{p}_{T,1}}{\frac{1}{L_{pp}} \int_{\mathbf{p}_{T,2}}^{\mathbf{p}_{T,2}/0.32} \frac{d^2 N_{pair}^{pp}}{dp_{T,1} dp_{T,2}} d\mathbf{p}_{T,1}}$$

$R_{AA}^{pair}(\mathbf{p}_{T,2})$ quantifies the suppression of the **subleading jet** in a dijet

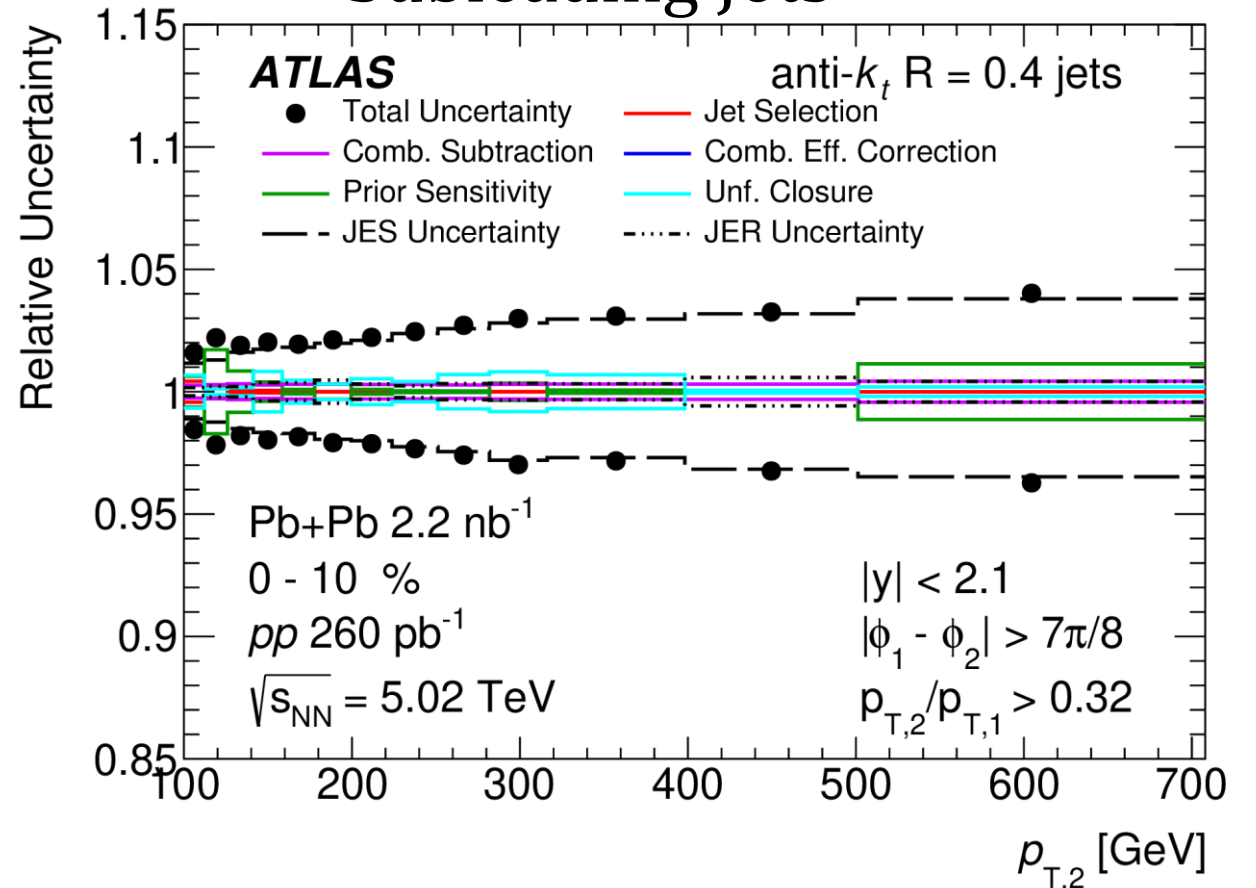
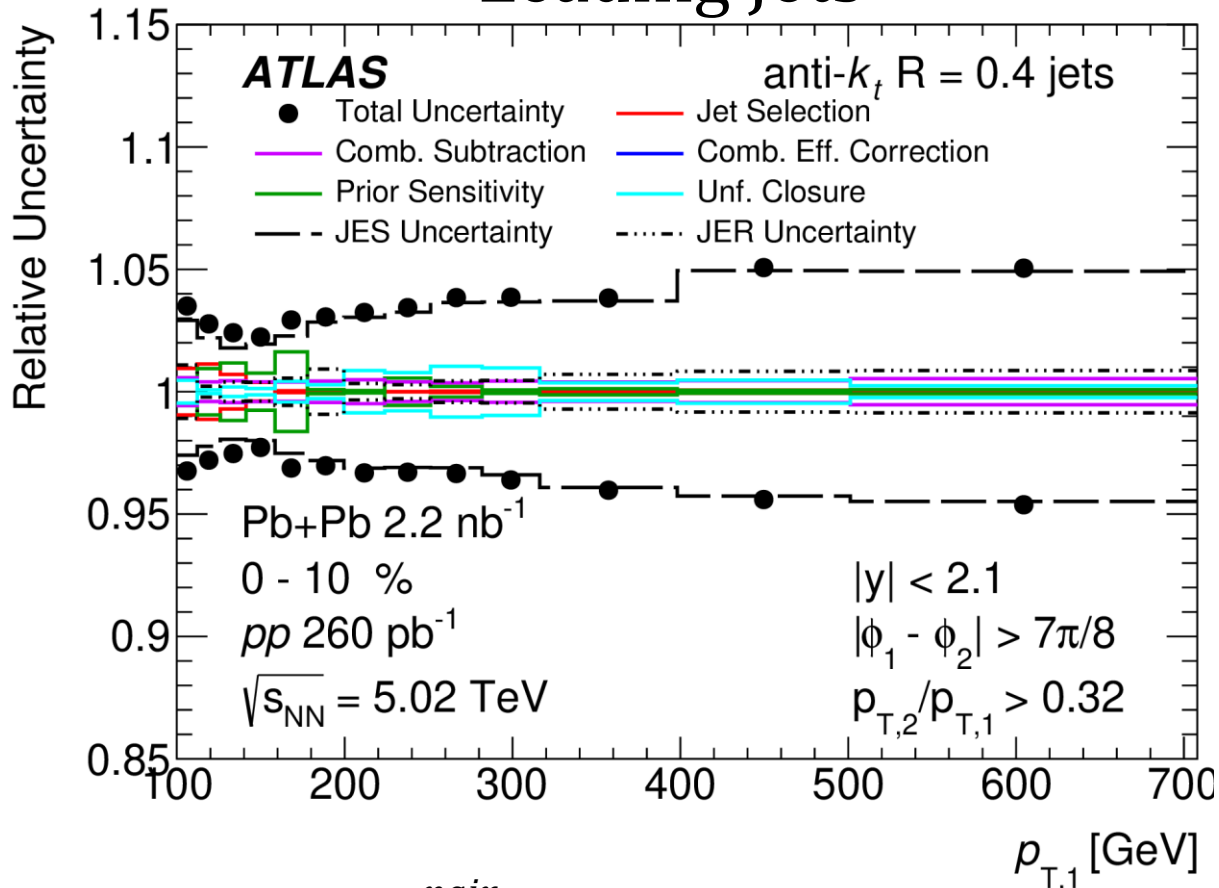

 $\frac{\mathbf{p}_{T,2}}{\mathbf{p}_{T,1}} > 0.32$

Dijet threshold condition of $\frac{\mathbf{p}_{T,2}}{\mathbf{p}_{T,1}} > 0.32$

Systematic uncertainties for R_{AA}^{pair}

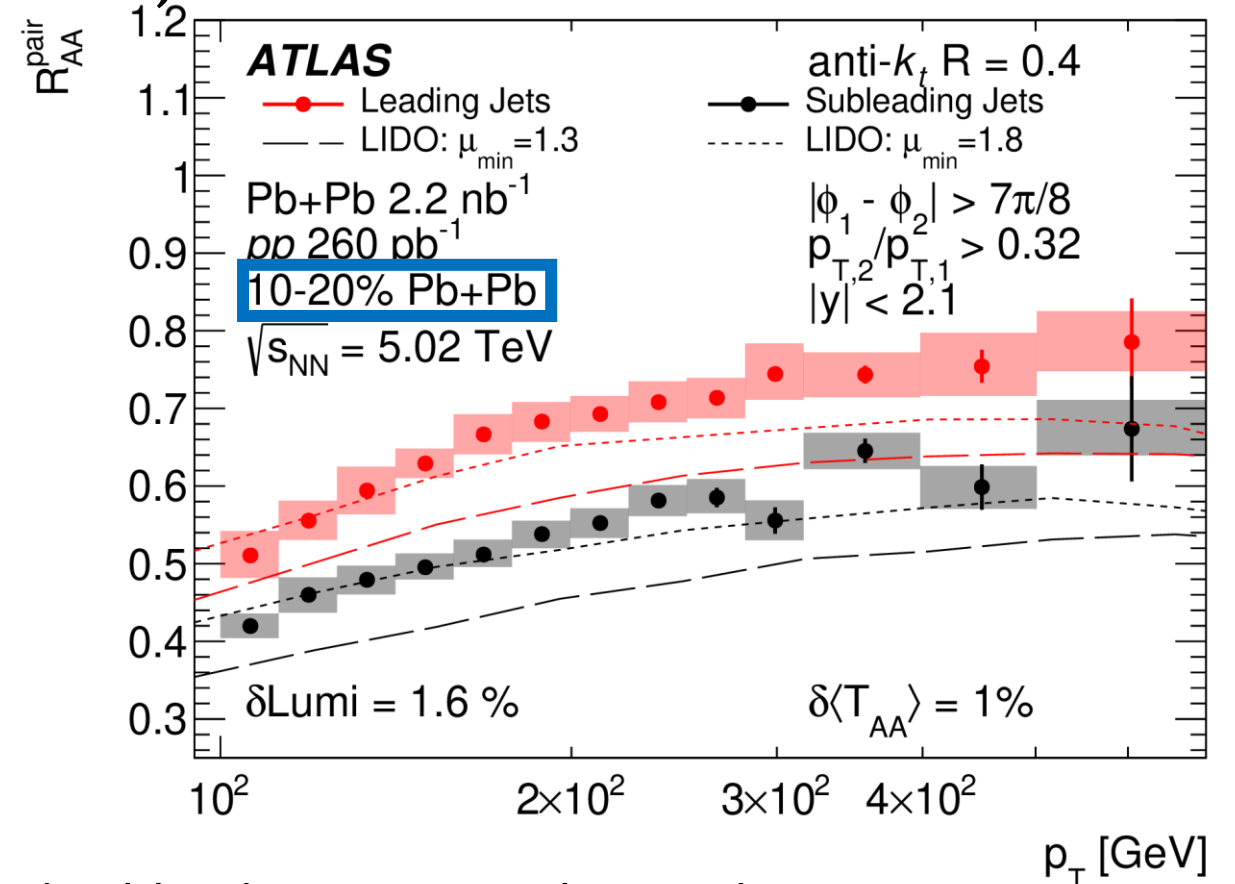
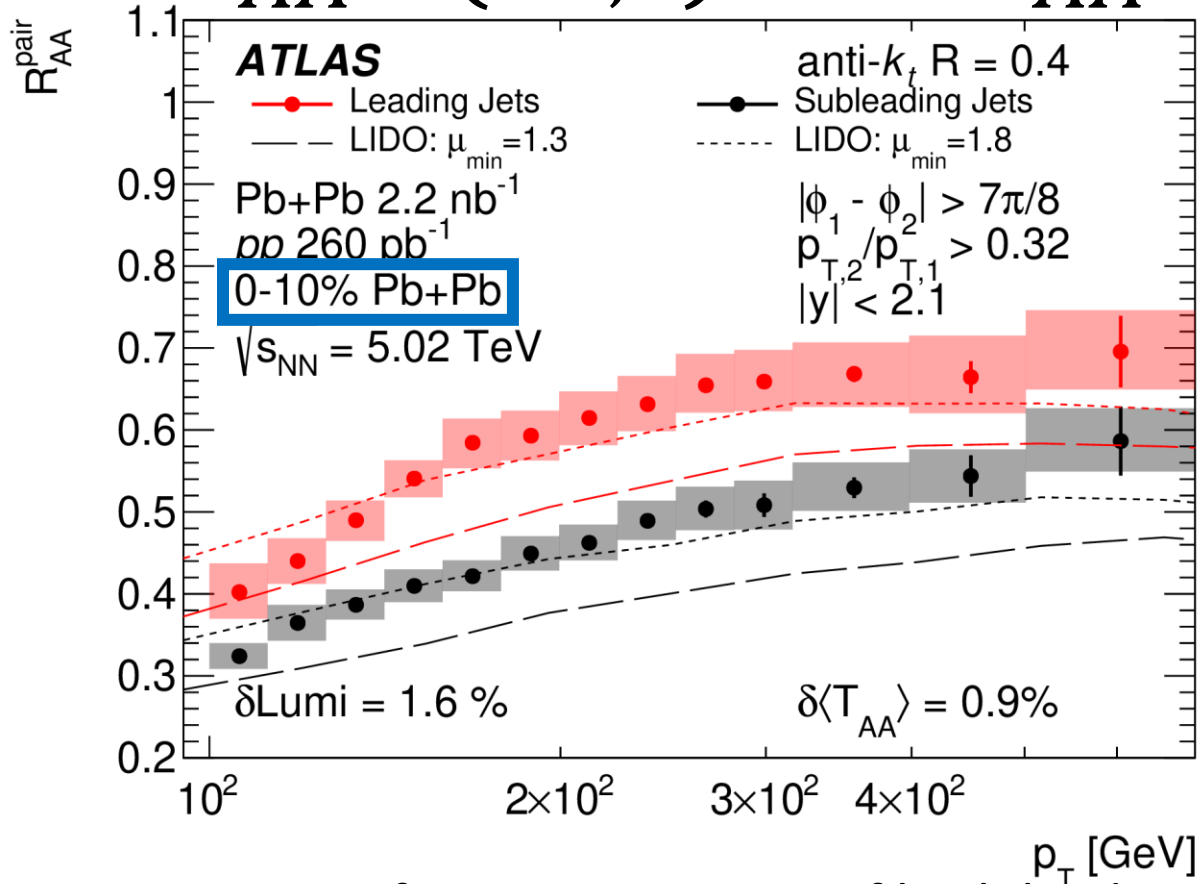
Leading Jets

Subleading Jets



For R_{AA}^{pair} the dominant sources of systematic uncertainty stem from uncertainty on the JES

$R_{AA}^{pair}(p_{T,1})$ and $R_{AA}^{pair}(p_{T,2})$



Significant suppression of both leading and subleading jets are observed across jet p_T

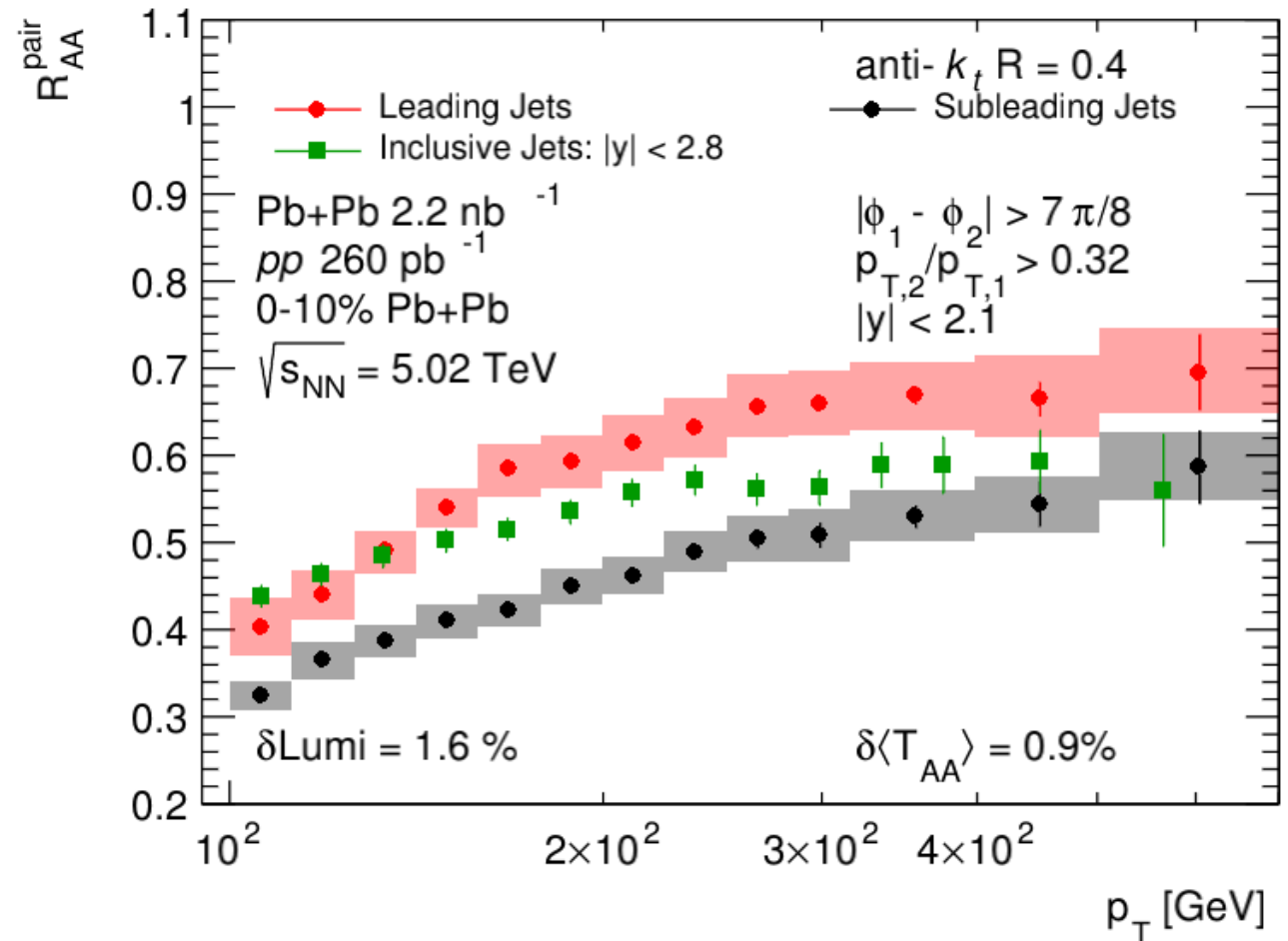
Subleading jets are systematically more suppressed than leading jets

$$R_{AA}^{pair}(p_{T,1}) \text{ and } R_{AA}^{pair}(p_{T,2})$$

Inclusive jet R_{AA} is sandwiched between leading and sub leading jets above 158 GeV

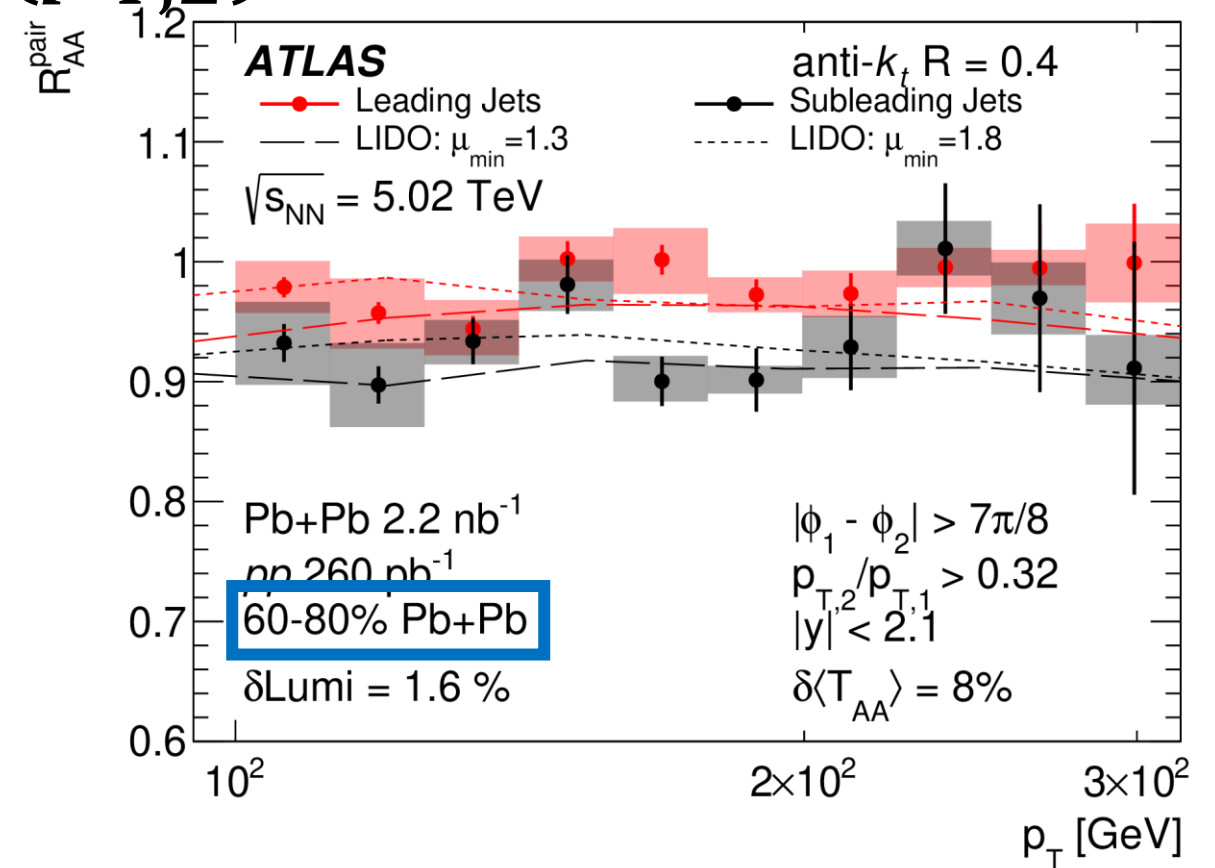
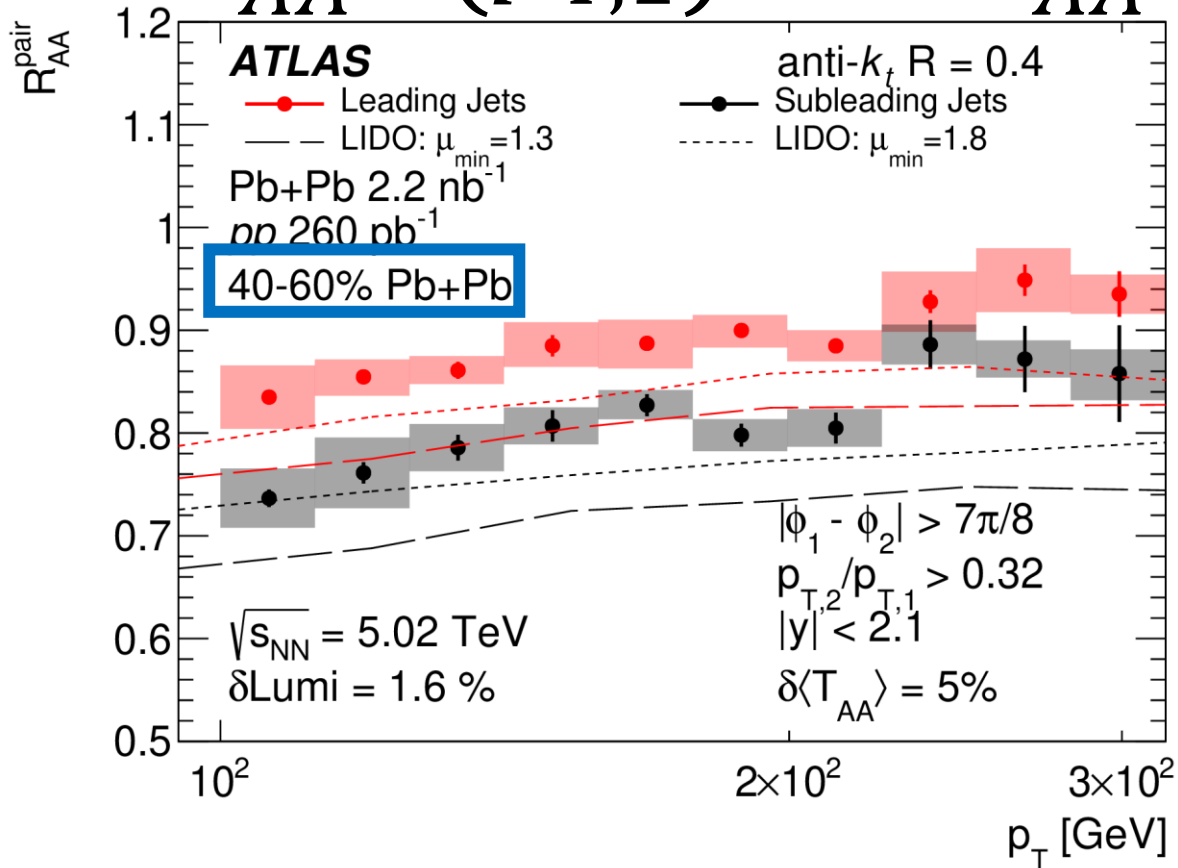
➤ Consistent with dijets dominating the inclusive jet spectrum

At low p_T the inclusive jet R_{AA} is above that of leading jets



Inclusive jets: <https://arxiv.org/abs/1805.05635>

$R_{AA}^{pair}(p_{T,1})$ and $R_{AA}^{pair}(p_{T,2})$



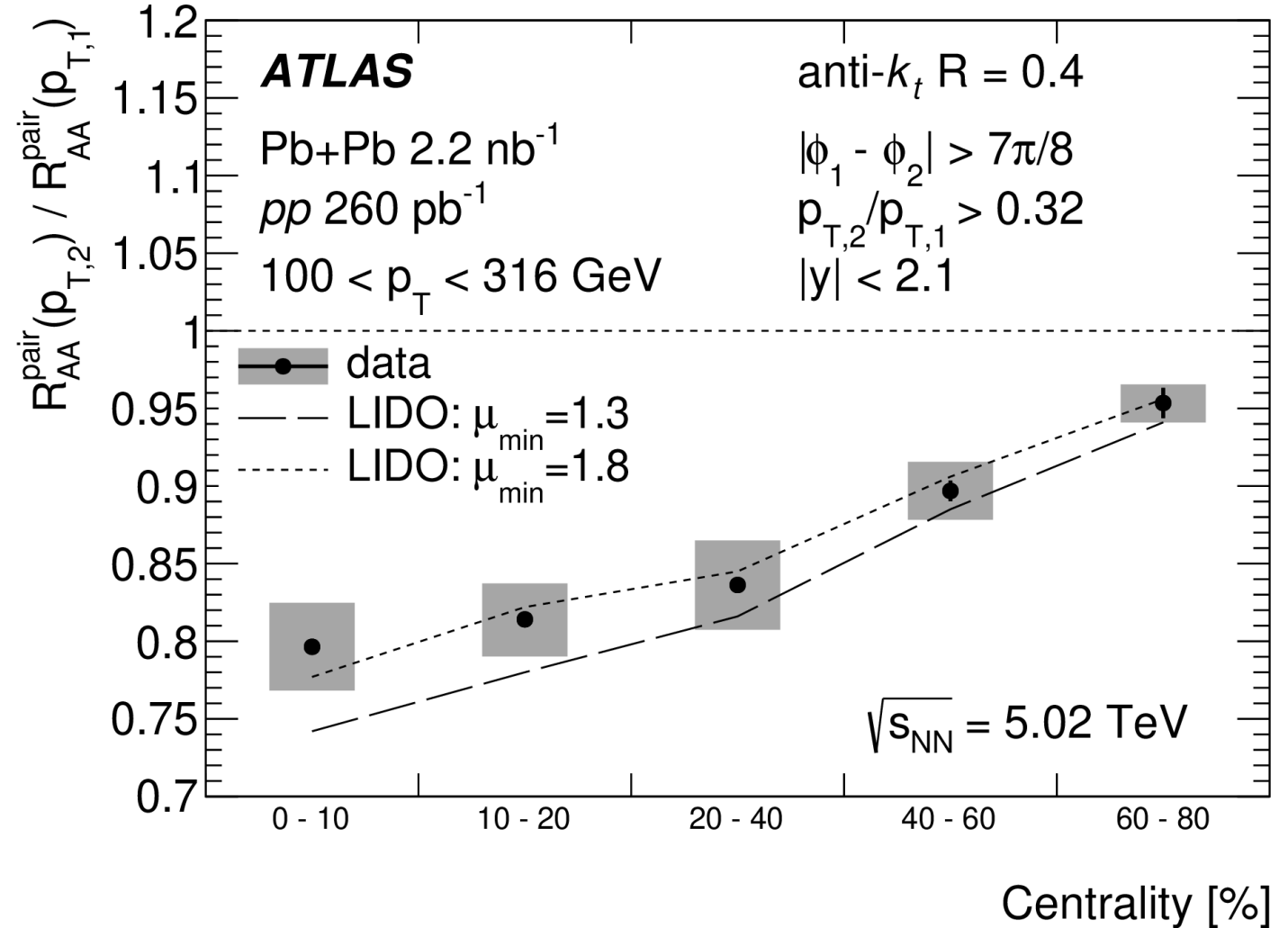
Systematic suppression of subleading jets relative to leading jets has been measured across event centrality

$$R_{AA}^{pair}(p_{T,2}) / R_{AA}^{pair}(p_{T,1})$$

Evidence for suppression of subleading jets relative to leading jets is observed

➤ 3σ significant relative suppression observed in peripheral Pb+Pb

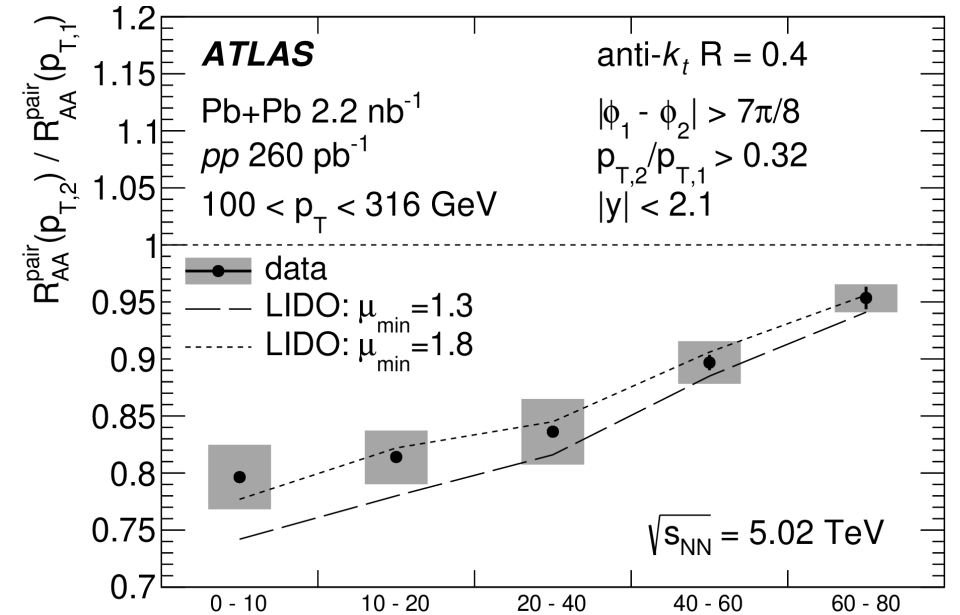
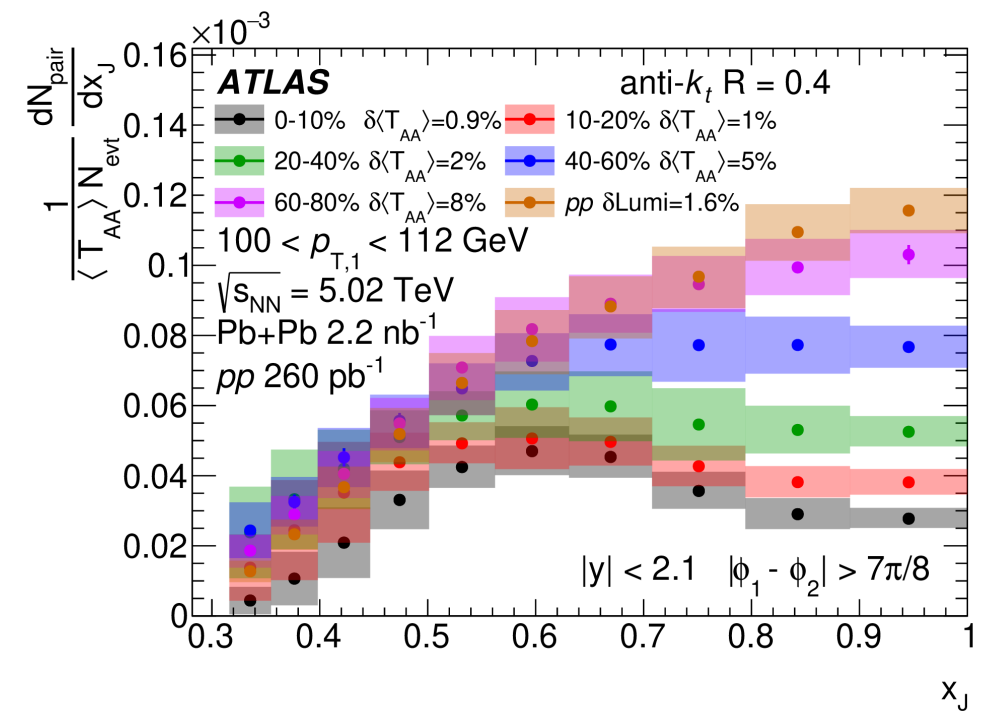
LIDO calculations with a $\mu_{min} = 1.8$ well reproduces the measurement



Summary

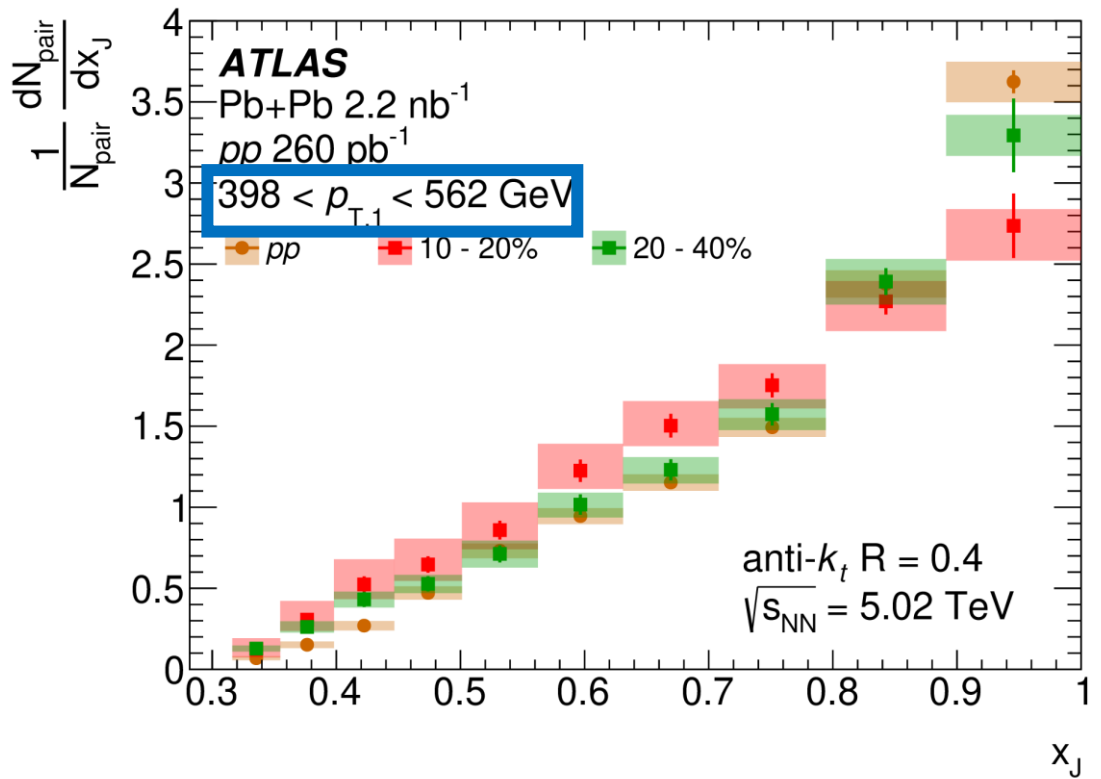
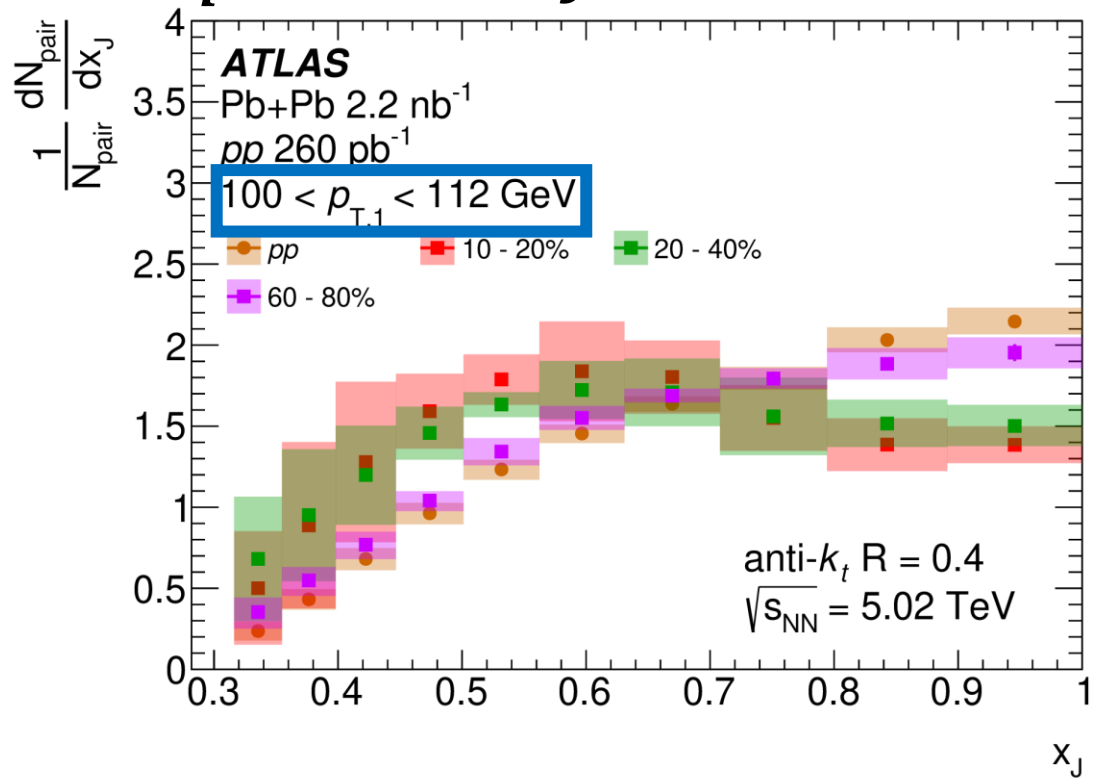
Novel measurements of dijets in Pb+Pb collisions have been presented

- Measurements of the absolutely normalized x_j distributions provide evidence of preferable depletion of balanced dijets
- Measurements of $R_{AA}^{pair}(p_{T,1})$ and $R_{AA}^{pair}(p_{T,2})$ quantify the suppression of leading and subleading jets
- A 3σ suppression of subleading jets to leading jets is observed in peripheral Pb+Pb



backups

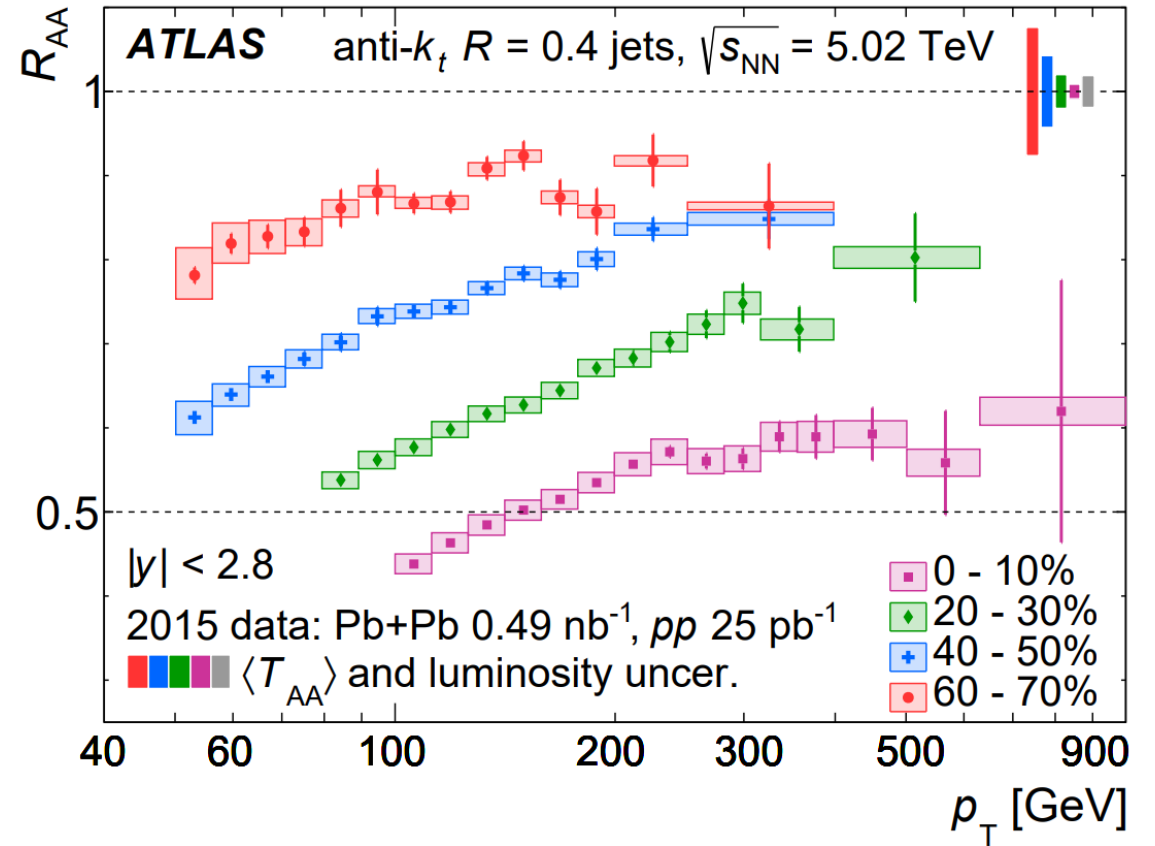
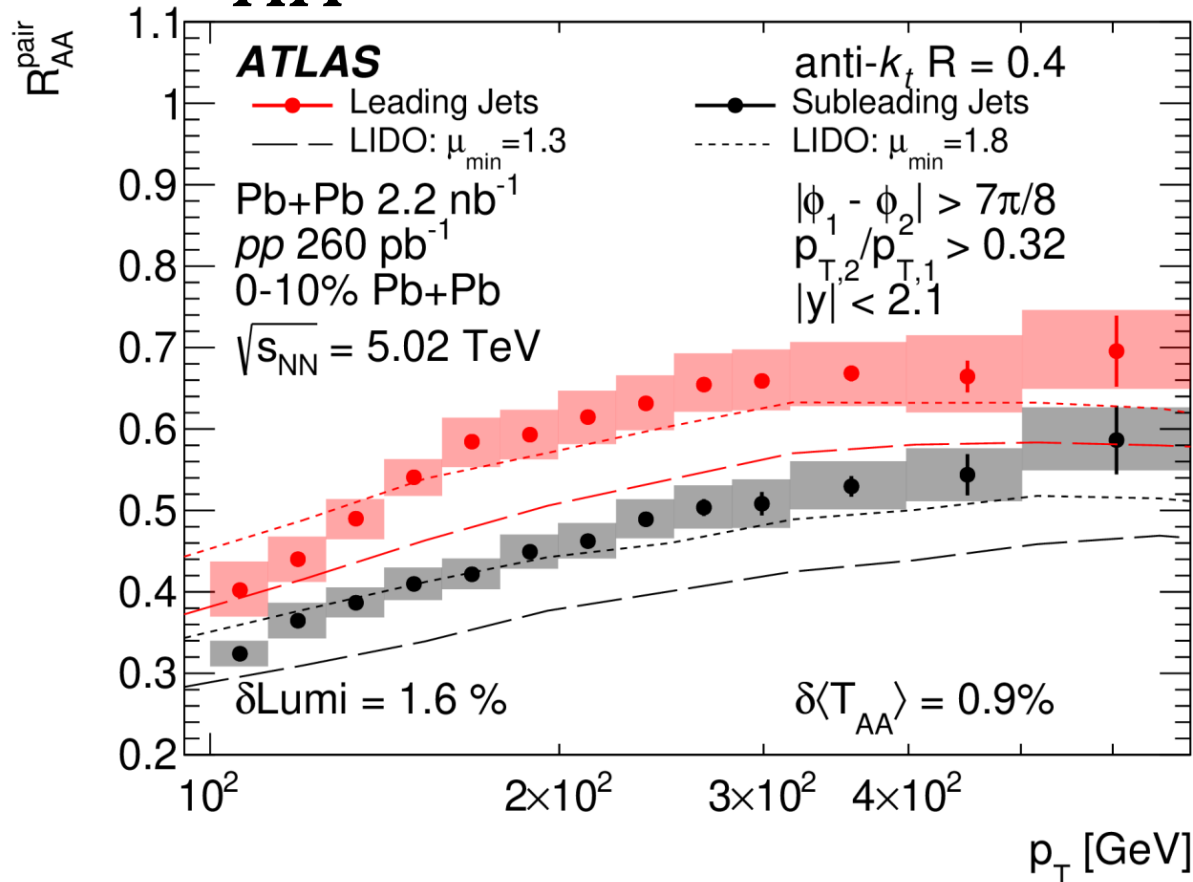
$\frac{1}{N_{pair}} \frac{dN_{pair}}{dx_J}$ additional centrality intervals



Significant modification from *pp* collisions in the x_J shape is observed across centrality at low $p_{T,1}$

Notable deviations from *pp* is observed up through 60% central Pb+Pb events for 398 < $p_{T,1}$ < 562 GeV

R_{AA}^{pair} and inclusive jets R_{AA} <https://arxiv.org/pdf/1805.05635.pdf>



The inclusive jet R_{AA} above 150 GeV is bracketed by the $R_{AA}^{pair}(p_{T,1})$ and $R_{AA}^{pair}(p_{T,2})$
 ➤ Below 150 GeV the inclusive jet R_{AA} is consistent with the $R_{AA}^{pair}(p_{T,1})$